UNIVERSITÀ DEGLI STUDI DI PADOVA

DIPARTIMENTO DI BIOLOGIA

Corso di Laurea magistrale in Biologia Marina

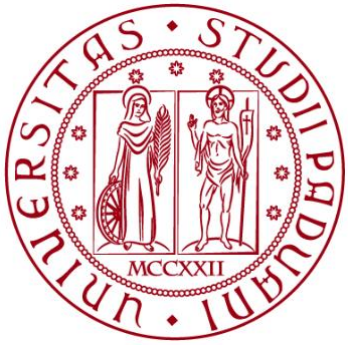

TESI DI LAUREA

Evaluation of fishery impacts on whiting (*Merlangius merlangus*, L., 1758): a historical comparison of life-history traits.

Relatore: Prof.ssa Carlotta Mazzoldi
Dipartimento di Biologia

Correlatori: Dott. Mario La Mesa
CNR-ISP di Ancona
Dott. Federico Calì
CNR-IRBIM di Ancona
Università di Bologna

Laureanda: Federica Stranci

ANNO ACCADEMICO 2021/2022

INDEX

1. INTRODUCTION

Fishing is a human activity that has been practiced for thousands of years, as a source of livelihood, especially for populations who lived near the coast or along rivers or lakes. The tools and equipment used, such as fish baskets, hooks and nets, initially rudimentary, have gradually become more specialized and efficient, capable of maximizing the catch of the species for which they were built. Yet, only in recent decades fishing has developed so much and in such a way as to cause profound changes in biodiversity and ecosystems (Cushing, 1988; Pauly *et al.*, 2002).

Jean Baptiste de Lamarck and Thomas Huxley, two of the foremost thinkers of the 18th and 19th centuries, believed that humanity could not cause the extinction of marine species. Their opinions reflected a widespread belief that the seas were an inexhaustible source of food and wealth of which people could barely use a fraction. Such views were given weight by the abundant fisheries of the time. Additionally, the incredible fecundity and wide distributions of marine fishes, combined with limited exploitation, provided ample justification for optimism (Roberts & Hawkins, 1999).

The fishing process became industrialized in the early 19th century (Pauly *et al.*, 2002) and further intensified over time, with the introduction of engines on fishing boats, as well as the replacement of plant fibers with synthetic ones for the construction of the nets, the introduction of deck auxiliaries (winches, windlasses, pole haulers, haulers, net winding drums) and electronic instruments (radar, GPS). Fisheries in the early 1950s were at the onset of a period of extremely rapid growth, both in the Northern Hemisphere and along the coast of the countries of what is now known as the developing world. Everywhere that industrial-scale fishing (mainly trawling, but also purse seining and long-lining) was introduced, it competed with small-scale, or artisanal fisheries (Pauly *et al.*, 2002).

Today, the evolution of sophisticated technologies still continues, also based on the greater knowledge of the behavior and biology of species of commercial interest. Jackson *et al*. (2001) recognized three different but overlapping periods of human impact on marine ecosystems: aboriginal, colonial, and global. Aboriginal use refers to subsistence exploitation of near-shore, coastal ecosystems by human cultures with relatively simple watercraft and extractive technologies that varied widely in magnitude and geographic extent. Colonial use comprises systematic exploitation and depletion of coastal and shelf seas by foreign mercantile powers incorporating distant resources into a developing market economy. Global use involves more intense and geographically pervasive exploitation of coastal, shelf, and oceanic fisheries integrated into global patterns of resource consumption, with more frequent exhaustion and substitution of fisheries. In some geographical areas, especially Africa, Europe, and Asia, these three cultural stages are strongly

confounded in time and space, so their differential significance is difficult to establish and a clear separation between these phases is difficult to implement.

The persistent and indiscriminate exploitation of marine resources, fueled by the growth of the world population and the increased demand for these goods on the market, has led over time to the decline, sometimes to the collapse, of entire fish stocks. In fact, reported world fisheries landings have been declining slowly since the late 1980s, by about 0.7 million tonnes per year (Pauly *et al.*, 2002).

The sharp decline in the abundance of some fish populations has therefore begun to manifest itself after years of overfishing. One of the most striking cases of commercial stock collapse involved Atlantic cod (*Gadus morhua*) in the early '90s, when most of the cod stocks off New England and eastern Canada collapsed, ending fishing traditions reaching back for centuries (Pauly *et al.*, 2002) and causing massive socio-economic damages. Abundance was so low for six of seven cod stocks that fishing bans of unspecified duration were imposed on commercial exploitation in 1992 and 1993. The causes were recognized in the overestimation of abundance and underestimation of fishing mortality, as well as the ability to catch fish efficiently at low abundance levels. The increase in fishing mortality was also associated with an underreporting fishery of older, legal-sized individuals (Myers *et al.*, 1997). Based on FAO's assessment (2020), the fraction of fish stocks that are within biologically sustainable levels decreased from 90% in 1974 to 65.8% in 2017. In contrast, the percentage of stocks fished at biologically unsustainable levels increased, especially in the late 1970s and 1980s, from 10% in 1974 to 34.2% in 2017. In 2017, among the FAO 16 Major Fishing Areas, the Mediterranean and the Black Sea had the highest percentage (62.5%) of stocks fished at unsustainable levels, followed by the Southeast Pacific (54.5%) and Southwest Atlantic (53.3%) (Figure 1).

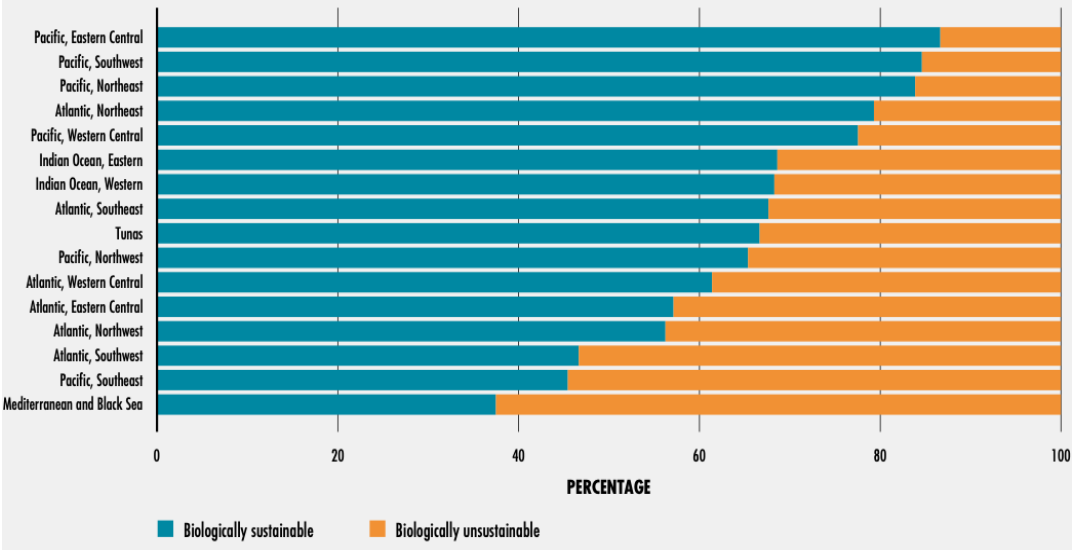

Figure 1. Percentage of stocks fished at biologically sustainable and unsustainable levels in 2017, by FAO statistical area (FAO, 2020).

1.1 Fishing in the Mediterranean and northern Adriatic Sea

The Mediterranean Sea is a complex region where ecological and human influences meet and strongly interact. While in the past the biodiversity of this basin has been shaped by geological and physical variations, today these are compounded by human activities and threats of different origin. The most important threats in this region are habitat loss, degradation and pollution, invasion of species, climate change and exploitation of marine resources, still the oldest and one of the most important maritime activities carried out by humans (Coll *et al.*, 2010). Evidence of negative effects of the Mediterranean resources exploitation dates back to very ancient times, firstly reported in the fourth century B.C. by Aristotle, who mentioned the disappearance of scallops from the main Greek fishing ground (Gulf of Kalloni, in Lesvos Island) since fishermen began using an instrument scratching the sea bottom (Voultsiadou *et al.*, 2010). The first records of overfishing and coastal resource depletion date back to Roman and medieval times, driven by the growth of the human population and the commercialization of food and products (Lotze *et al.*, 2006; Gertwagen *et al.*, 2008).

The current high demand for marine resources continues and has resulted in high levels of fishing or harvesting intensity (Coll *et al.*, 2010). A fleet of about 73,000 vessels is operating along the Mediterranean coasts (Colloca *et al.*, 2017). In areas exploited more sustainably (e.g., Gulf of Gabes, Eastern Ionian, and Aegean Sea) fishing pressure was characterized by either a low number of vessels per unit of shelf area or the large prevalence of artisanal/small-scale fisheries. Conversely, GSAs in the Western Mediterranean Sea and the Adriatic Sea showed very low ecosystem sustainability of fisheries that can be easily related to the high fishing pressure and the large proportion of overfished stocks obtained from single-species assessments. According to the General Fisheries Commission for the Mediterranean (GFCM, 2016) data, the temporal trend in annual production of demersal fish, crustaceans, cephalopods and small pelagics showed a rapid increase from the 70s to the beginning of the 90s followed by a declining trend since then.

Looking at the state of the area considered for this thesis and at the exploitation of its fish stocks, the northern Adriatic Sea is undergoing several anthropogenic pressures and high environmental variability. It is considered the most exploited basin of the Mediterranean Sea (Caddy *et al.*, 1995; Barausse *et al.*, 2009), given its shallowness (max 35 m), the semi-enclosed geographical configuration, the characteristic presence of incoherent sediments, and its high productivity. These elements make it a flat trawlable platform, where more than 15% of the Italian fishing activities are concentrated (Pranovi *et al.*, 2015).

Time series of fishery landings can provide indications of changes in both community abundance and composition (Fiorentino *et al.*, 1997; Pauly *et al.*, 1998, 2002) and are, therefore, useful tools for understanding the impacts of anthropogenic and natural factors on marine ecosystems. However, it is important

to remember that these data can reflect actual changes in stocks only partially, as several factors can influence landing trends.
In the northern Adriatic Sea, the local landings of the Chioggia fleet can give some indications about the stock state in this area. It seems that even if the total landings increased during the last decades, the ratio of total landings to fishing capacity showed a negative trend. Moreover, the evenness of the landings decreased over the last few years, indicating the dominance of a few species, and community life-history traits changed: landings revealed a general decline in maximum age and size, and in age and size at sexual maturity, as well as an increase in fecundity. The observed trends are likely to mirror a relative decrease in large-sized, long-lived, late- and large-sized-maturing species, and a relative increase in more fecund ones. The total landings and landing composition were influenced also by environmental factors. In fact, river runoff may change salinity or enhance nutrient loads, and exceptional events, such as anoxic phenomena, and eutrophication trends, have probably also been involved in these observed shifts in landing composition (Barausse *et al*., 2011).
There is an increased concern about the status of the Mediterranean ecosystem in relation to the sustainability of the current level of fisheries exploitation (Colloca *et al.*, 2017). The rapid warming, combined with the expansion of non-indigenous species is definitely changing the suitability of the habitats for traditional commercial species, with effects on their resilience to fishing (Libralato *et al.*, 2015).

1.2 Life-history traits and population dynamics

The ways how evolution designs organisms to achieve reproductive success is what life-history theory tries to clarify. It aims to explain variation in size at birth, growth rates, age and size at maturity, clutch size and reproductive investment, mortality rates and lifespan – all defined as life-history traits (or 'tactics' [Stearns, 1976]). The evolutive processes of life histories are related to the environment and to how it affects the survival and reproduction of organisms of different ages, stages, or sizes (Stearns, 2000). This theory is based on optimization models and on fitness maximization. To better understand this concept, longevity and attainment of big sizes or, on the contrary, a very short life can be seen as different consequent strategies for responding to environmental pressures, for instance to heavy predation exposition. A short life span means precluding the attainment of large size, requiring early maturity, probably a higher birth rate, and increasing the possibility of mortality from physiological exhaustion**.** As another example, within this framework, iteroparity may be considered an evolutionary response to uncertain survival from zygote to first maturity (Murphy, 1968), therefore a strategy aimed at increasing the probability that at least a certain number of individuals may reach the sexual maturity and reproduce.

Overfishing has caused dramatic changes in the structures of exploited populations as well as ecosystems (Hsieh *et al.*, 2010). The vulnerability to fishing pressure of different species is strictly related to their life-history traits. Jennings *et al*. (1998) pointed out that fish stocks' tendency to decline more than expected from their rates of fishing mortality is especially in those species having high ages at maturity, large maximum size, and low potential rates of population increase. Larger and later maturing species are less able to withstand a given rate of fishing mortality than smaller earlier maturing ones. This suggests that small and early maturing species would increase in relative abundance in an intensively exploited multispecies fishery. However, also in these cases, the shorter reproductive lifespans of these species may lead to instability in population size, placing the species in the same danger of decline. It is also important to underline that maturity and growth parameters of fishes are closely interrelated because of the trade-offs among life-history traits allocations (Stearns, 1976), and the overall output of these trade-offs influences the response to exploitation.

Fishing pressure, overexploitation of populations as well as environmental changes determine modifications on life-history traits too, modifying the structure of the exploited population. Fishing, in addition to simply removing biomass, also truncates the age and size structure of fish populations, often resulting in localized depletions, because fisheries usually target and/or selectively remove large and therefore old individuals (Berkeley *et al.*, 2004). A long-tailed age structure (a long tail of old individuals in the age distribution) certainly provides a higher reproductive output (Hsieh *et al.*, 2010). In addition to this reason, other biological effects associated with a long-tailed age structure include (1) age-related differences in spawning locations and time, and (2) increased quantity and/or quality of eggs produced by older (experienced) or larger fish (Hsieh *et al.*, 2010). A larger population of shorter-lived fish requires a higher intrinsic rate of growth; the population must produce more surviving offspring per capita per year to compensate for the shortened life span (Hsieh *et al.*, 2010).

So, the average age (size) of a targeted and overexploited population is usually reduced (Hsieh *et al.*, 2010) and this seems to have further consequences on populations' structure. For instance, an analysis carried out by Anderson *et al.* (2008) suggested that the increased temporal variability in the of Californian exploited fish stocks does not arise from variable strength of the exerted exploitation pressure, nor does it reflect direct environmental tracking: more likely, it comes from an increased instability in population dynamics. This has implications for resource management, as selective harvesting can alter the basic dynamics of exploited stocks, and lead them to unstable booms and busts that can precede systematic declines.

Knowing the age of fish populations is essential to understand the dynamics of fish stocks (Cooper, 2006; Haddon, 2011; Maunder & Piner, 2014). Fish ages are

routinely used, together with measurements of length and/or weight, in determining population/stock composition (in respect of size and age), age at maturity, maximum life span/longevity, mortality, and production. Performing an age structure analysis is also important for examining variations in growth rate within a population and across a species' range, and as a key parameter in population dynamics estimates. With age analysis studies it is possible to better model the current and future impacts of fishing pressures and environmental stresses on the species' different life stages; the impacts on adult spawning populations and those on recruitment phase, being of particular importance to manage the stocks (Proctor *et al.*, 2021). The basic population dynamics model assumes that mortality, both natural and fishing-related, affects all fish equally. Actually, fish of different ages experience different rates of mortality. When appropriate data, such as valid length-age keys, are available, the population can be separated into age classes. In an age-structured model, separate mortality rates exist for each age class, and the number of recruits is only relevant to the first age class (Figure 2; Cooper, 2006).

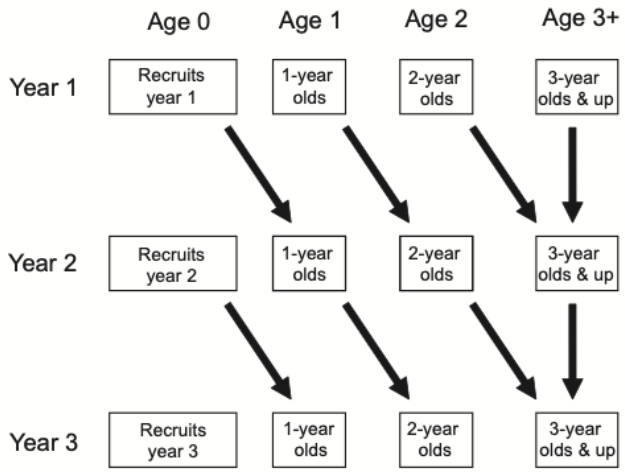

Figure 2. Diagram illustrating an age-structured population dynamics model, with a plus-group that starts at age 3. The plus group contains all fish age 3 and older (Cooper, 2006).

The structures most commonly used to age fish are otoliths, vertebrae, scales and spines. Otoliths are the most widely used structure for ageing fish, primarily because, in general, the growth zones are more clearly defined and hence more easily 'read' than those in vertebrae, scales and spines. Some studies have shown that ageing by scales or spines can yield under-estimates in age for older fish compared to those obtained from otoliths. Otoliths are generally more easily removed from the fish and easier to prepare for reading compared to vertebrae. Scales, and perhaps to a lesser extent spines, have a significant disadvantage of being structures that can be lost, eroded or damaged and replaced during the lifetime of a fish and therefore ages determined from scales may not reflect the full age of

the fish. In contrast, otoliths are internal structures growing in size during the entire fish's lifetime (Proctor *et al.*, 2021).

1.3 Otoliths

1.3.1 General description

The inner ear, which is found in all jawed Vertebrates, functions both as an auditory system, that detects sound waves, and a vestibular system, which detects linear and angular accelerations, enabling the organisms to maintain balance. In fish, the inner ear is a paired structure embedded in the cranium on either side of the head, close to the midbrain. Each ear is a complicated structure of canals, sacs, and ducts, filled with endolymph, a fluid with special viscous properties. In Osteichthyan species the inner ear presents three otic sacs, each containing a calcareous structure, an otolith, that acts as a mechanoreceptor stimulating the kinocilia ("hair" cells) of the *macula*. The three otic sacs are the *sacculus*, *utriculus* and *lagena*, which contain the *sagitta*, *lapillus* and *asteriscus* otoliths, respectively. Each otolith is fixed over the *macula* by an otolithic membrane, into which sensory cilia project. The otoliths of the three otic sacs differ in size and shape (Figure 3; Panfili *et al.*, 2002).

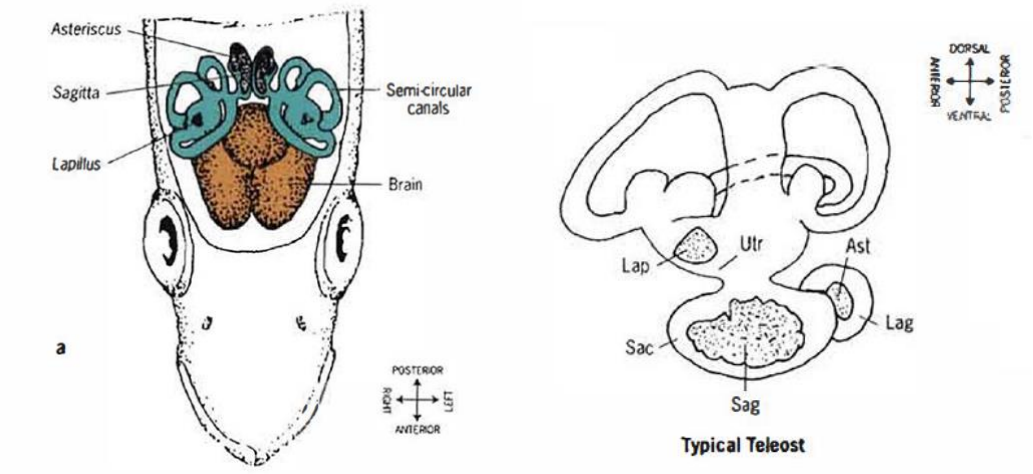

Figure 3. Left: Dorsal view of the vestibular apparatus in a typical Teleost species. The top of the cranium is cut away (frontal section). Right: Otoliths within the labyrinth systems of typical Teleost fish (Panfili *et al.*, 2002).

Otoliths are formed extracellularly from the crystallization of the aragonite form of calcium carbonate onto an organic matrix template composed largely of a keratin-like protein called otolin. The otoliths accrete by the addition of concentric layers of proteins and calcium carbonate (Panfili *et al.*, 2002).

1.3.2 Periodic increments and age estimation

Calcified structures in fish, as otoliths, grow throughout the life of the individual and act as a permanent record, a trace of episodic patterns of growth at different timescales. So, it is possible to relate these processes to time, for example determining length-at-age, fishing mortality by year, maturity-at-age, etc., all important parameters for stock assessment. In particular, otoliths exhibit a range of incremental structures that are often formed regularly over time scales ranging from sub-diurnal to annual. They appear to be highly suitable for age estimation, which depends on visible changes in otoliths' growth (Panfili *et al.*, 2002).
The growth patterns of most interest are at four levels of resolution:

- Primary increments, permitting a resolution of days;
- Seasonal zones, permitting a resolution of several months or a growth season;
- Annual increments, permitting a resolution of years;
- Discontinuities in the otolith (ultra)structure, which correspond to various stresses that were not necessarily regular during the life-history of the individual.

Seasonal increments, also termed seasonal zones, marks, rings or *annuli*, are often distinguishable on otoliths, in both whole/untreated otoliths or after some form of preparation (Panfili *et al.*, 2002), as an alternation of hyalin and opaque bands.
Seasonal zones can reach a few hundred microns in width and are therefore visible to the naked eye or at low magnifications (10x-40x). The difference in the organic matrix content of the two zones can be underlined after burning which turns the organic matrix a rich opaque brown, or after staining, which colours the chromophilic organic zones (Panfili *et al.*, 2002).
The identification of seasonal increments, however, can be difficult due to the presence of false or split rings and discontinuities, that correspond to non-seasonal events (migrations, spawning). Identification is based on their distinctiveness, their continuity around the otolith, their thickness and their relative width. These should decrease in width from the central parts to the edge of the otolith, in line with the fall in rates of growth with age.
A reader can establish the age of the fish by simply counting the number of seasonal increments on an annual basis. As in the case of specific age estimation, other information should also be taken into account: date of capture; the peak spawning period for a given population (precise or average or standard population date of birth); main periods of seasonal increment formation; the nature of the otolith edge (Panfili *et al.,* 2002).
In order to be able to establish the age group/class to which the fish belongs, it is necessary to count the number of annual increments from the centre towards the

outer edge of the otolith. If the date of capture is known, it is possible to calculate the year in which the fish was born. The ability to estimate the age of the fish from otolith may directly support the determination of lifespan or longevity in individual fish populations and species.

Indications about life-history events can be found studying otoliths or other calcified structures: age at maturity and reproduction event, lifespan/longevity, and migration.
Reproduction places a severe energy demand on fish, and after the onset of sexual maturity there may be a reduction in somatic growth in favour of energy storage for reproductive activity. This affects the growth of calcified structures, and the influence of reproductive activity is often recorded permanently in scales and otoliths (called "spawning checks" by Williams & Bedford, 1974). However, since translucent formation is mineral-rich and protein-poor and since feeding activity in several species is also reduced during the final stages of gonad maturation and spawning, this may influence the rate of protein synthesis available for otoliths as well as for other tissues and result in the observed translucent structures (Panfili *et al.,* 2002).
Many fish species move between different water masses during their ontogeny undergoing severe habitat shifts (eg. seasonal migration), that consist of a long-term or permanent move into new waters. Information about the timing of these migrations can be found through the examination of the changes in the appearance of increments in otoliths. For instance, the pattern of otolith increments is often used to identify the timing of catadromous migrations in eels. The composition of otoliths also changes when fish move into new environments and this can be used to obtain detailed data about fish age at migration and the duration of the transition between different environments (Panfili *et al.*, 2002).
Finally, otoliths have a species-specific shape and size. This makes them useful tools for species identification in some peculiar cases, such as during the study of stomach contents, when fish preys result partially or mostly digested.

1.3.3 Validation methods

The temporal meaning of the observed patterns must be determined in order to evaluate the closeness of the estimated age to the accurate age of the fish (Panfili *et al.*, 2002). Validation studies are fundamental in fish age estimation because they provide accurate mortality and growth rate estimates for stock assessment. Moreover, validation is important to avoid errors in age estimation, which will especially affect the estimates of recruitment, fishing mortality, and spawning-stock biomass. To validate the age estimation method (i) the increments must be laid down with a periodicity that can be related to a regular timescale (i.e. accuracy) and

(ii) the age estimation structure must have a consistent interpretable pattern of increments (i.e. precision) (Vitale *et al*., 2019).

There are several validation methods that can be used and it is possible to classify them as 1) direct validation method, that is individual-based technique which makes use of precise temporal reference marks on the calcified structure. In this case the validation is based on tag and recapture of the same individual, and this can be done with different techniques and markers. An alternative direct method is to rear the individuals in captivity. The 2) semi-direct validation methods are based on the observation of the otolith marginal zones evolution over time. Marginal increment analysis, edge-zone analysis, daily increment analysis, microchemistry (tracking the seasonally varying incorporation rates of different microconsituents and stable isotopes) are all methods belonging to this category and differ from the 3) indirect validation methods, which are based on length-frequency information. Length-based methods analyse the length composition of catch landings in order to identify the various age-groups present, based on the assumption that each age group has a normally distributed length composition and a different modal length. So, age 0 corresponds to the smallest mode present in the sample obtained after the spawning period, while subsequent modes correspond to age 1, etc (Panfili *et al.*, 2002; Vitale *et al.*, 2019).

The edge-zone analysis and the marginal increment analysis (MIA) are among the most frequently employed validation methods (Campana, 2001; Goldman, 2005). These methods focus on incremental patterns of growth rings throughout one whole year. They assume that, if growth bands are formed annually, the width or the density of the edge increment will exhibit a yearly sinusoidal cycle when plotted against the month of capture. The edge-zone analysis, used for this work, is a qualitative assessment of the relative opacity and translucency of the edge of the age structure (Okamura *et al.*, 2013). Edge analysis does not assign a state of completion to the marginal increment, but rather records its presence as either an opaque or translucent zone. When the relative frequency of each edge zone is plotted across months or seasons, the cycle frequency should equal one year in true *annuli* (Campana, 2001).

1.4 Study species: Whiting, *Merlangius merlangus*, L., 1758

1.4.1 Biology of whiting

Figure 4. *Merlangius merlangus*. © Scandinavian Fishing Year Book.

Phylum: Chordata
Class: Actinopterygii
Order: Gadiformes
Family: Gadidae
Genus: *Merlangius*
Species: *Merlangius merlangus*

Whiting, *Merlangius merlangus* (Figure 4), the only species of the genus *Merlangius*, is a fish distributed in the north-eastern Atlantic, in the North Sea, in the Mediterranean (limited to the coasts of the north Aegean, the Adriatic and the Tyrrhenian Sea) and in the Black Sea (Vallisneri *et al.,* 2004).
Morphologically, the body appears rather tapered and compressed at the sides. The chin barbel is absent or very small and the upper jaw slightly projects. On the top, three dorsal fins are present and separated by small spaces. Two anal fins touch each other or nearly so; the anterior anal fin base results elongate, one-half or more of preanal distance; the pectoral fins reach well beyond the origin of the anal fin; the pelvic fins have a slightly elongated ray. The lateral line is continuous along its entire length. Lateral-line canals are also present on head with pores. The colour is variable, often a small dark blotch at upper base of pectoral fin is visible (Cohen *et al.,* 1990).
It is a benthopelagic species, usually living at depths from 10 to 200 m, but more common from 30 to 100 m, mainly on mud and gravel bottoms, but also on sand and rocky bottoms. Juveniles are found in shallower waters**,** from 5 to 30 m depth. Only after the first year of life whiting usually migrates, leaving the nursery areas for the open sea (Cohen *et al.,* 1990).
This species prefers cold waters, so that its distribution is – in the Mediterranean Sea – more northerly than other species of Gadidae. It is indeed very common in the northern and central Adriatic Sea, where in winter the shallowness and the cold

Bora wind, make the mean temperature of the water very low. In this sense, the Adriatic Sea is quite different from the other Italian seas and Mediterranean areas for the presence of species with a northernmost distribution areal which are absent elsewhere, for example whiting, sprat (*Sprattus sprattus*), and European flounder (*Platichthys flesus*). These and other species might be the proof of Atlantic fauna penetration in the Mediterranean Sea from temperate-cold climates that happened during the glaciations (Pleistocene). These species would have survived in the north Adriatic Sea thanks to the peculiar features of this basin (Bombace & Lucchetti, 2002).

The diet of adults includes small crustacea (mainly decapods), molluscs, small fish, polychaetes, and cephalopods (Cohen *et al*., 1990; Stagioni *et al.*, 2008). This species shows sexual dimorphism in the growth rate, which is higher in females, being able to reach bigger sizes compared to same-aged males (Vallisneri *et al.*, 2004). The maximum size ever reported is 91.5 cm, in the North Sea (Wilhelms, 2013), whereas in the Adriatic Sea the maximum size reported in literature is 42 cm (Bolognini *et al.*, 2013).

Probably, in the Adriatic Sea, sexual maturity is reached at the end of the first year of life, corresponding to a total length of about 20 cm (Giovanardi & Rizzoli, 1984). Whiting is a batch spawner species: the reproductive period recorded for this species in the Adriatic Sea is wide, lasting from November to May, with a peak in December (Vallisneri *et al.,* 2004). The spawning area corresponds to the adults' distribution area (Giovanardi & Rizzoli, 1984).

Beyond the population of the Adriatic Sea, it is necessary to consider the other ones, mainly distributed in the Black Sea, North Sea, and northeast Atlantic Ocean. Among these populations, there are some significant differences in the growth rate, maximum size, maturity size, spawning periods, and number of age classes of the population. At higher latitudes, the whiting appears to reach sexual maturity at larger sizes than the Adriatic population. In particular, Cooper (1983) reported a length of first sexual maturity of 27.5 cm for females and 25.5 cm for males in the Scottish Atlantic Ocean. In the North Sea, most whiting mature by age 2 (Gonzales-Irusta & Wright, 2017). In the Black Sea, instead, the sexual maturity seems to be reached at a smaller size, namely at 13.9 cm for females and 12.5 cm for males, as reported by Yildiz *et al.* (2022).

In the North Sea, multiple spawning peaks occur during the spawning period, that extends from January until June (Gonzales-Irusta & Wright, 2017). In the Atlantic Ocean, along the Scottish coasts, spawning is more limited in time and begins later, occurring between March and June (Cooper, 1983). In the Black Sea, Mazlum & Bilgin (2014) reported an extended period of spawning throughout the whole year, with three peaks in February, April and November.

As a commercial species, in the Mediterranean Sea whiting is caught mostly by trawling, even if the bigger individuals can be captured with longlines. The highest

catches are attained in the north Adriatic Sea, at the mouth of the Po River, especially in winter, when the new recruits join the adult stock. Whiting is generally captured in association with other species, such as the poor cod, *Trisopterus capelanus* (Bombace & Lucchetti, 2011).
M. merlangus is intensively captured especially in the North Sea. In this area it becomes a target species only in some part of the year, but generally, it represents only a by-catch species of bottom trawling activities (Bombace & Lucchetti, 2011). It is usually marketed fresh, as chilled fillets, frozen, dried-salted, and also used as feed for the Black Sea-trout (Cohen *et al.*, 1990).

1.4.3 Whiting ageing

In *M. merlangus* the otoliths are of large size, with a typical lanceolate shape, and characterized by the presence of bumps (Figure 5). The latter are particularly evident in some specimens, and typically more accentuated in the small ones. On the convex, proximal side of the otolith, a slight depression is visible corresponding to the *sulcus acusticus*.

Figure 5. Whiting's otoliths. *Above*: proximal side of the otolith, it is visible the *sulcus acusticus*. *Below*: distal side of the otolith.

In the cross sections, the acoustic sulcus is configured as a structure with a triangular shape. It is to be noted that this study species and, more generally, the species belonging to the Gadidae family usually present large-sized otoliths which continuously thicken as they grow. The thickness and the opacity of these otoliths make it very difficult to read them as a whole, especially hindering the observation of the nucleus or the early growth zones (Panfili *et al.*, 2002). For this reason, inner structure readability may be further improved processing the otolith by several techniques, as staining (Richter & McDermott, 1990), cross sectioning (Tomas, 2006; Polat & Gümüs, 1996, Dufour *et al.*, 2020), sagittal sectioning (Ross & Hüssy, 2013), burning (Polat & Gümüs, 1996). About burning the otoliths, heating

until their protein denatures turns brown in colour. This renders the winter, translucent growth zones more visible (Panfili *et al.*, 2002), intensifying the contrast between the rings and facilitating the age estimation.
It is possible in some cases to identify, exclusively at the level of cross section, in the dorsal part of the otolith, depositions similar to the opaque ones within a hyaline ring. These depositions are called "Humphries shadows" and are typical features of whiting otoliths. The appearance is not the same as that of the "real" rings: the outline is less defined, the shape is that of an inverted "C", and the observations of the color camera show that the color is not the same as that of a matte ring. The problem is that these Humphries shadows are in the reading axis and fit between the real rings, creating issues during the age readings. However, they are only detectable in the dorsal part of the otolith (the longer and thinner of the cross section), unlike the rings which are visible anywhere in the section (except at the acoustic sulcus). Their distinctive appearance and position usually avoid confusion during age reading (Dufour *et al.*, 2020).

1.4.2 Whiting landings

FAO landings data related to this species in the Mediterranean Sea (available from 1970 to 2018) show a general decrease after the two successive peaks reached in the late 70s and 80s (Figure 6). It is important to note that almost all of the landings came from the Black Sea (about 76% of the total landings in 2018). Furthermore, the data relating to the Adriatic Sea unfortunately only began in 1998 and data collection was scanty until 2005, even if the species has a quite commercial relevance in some local markets.

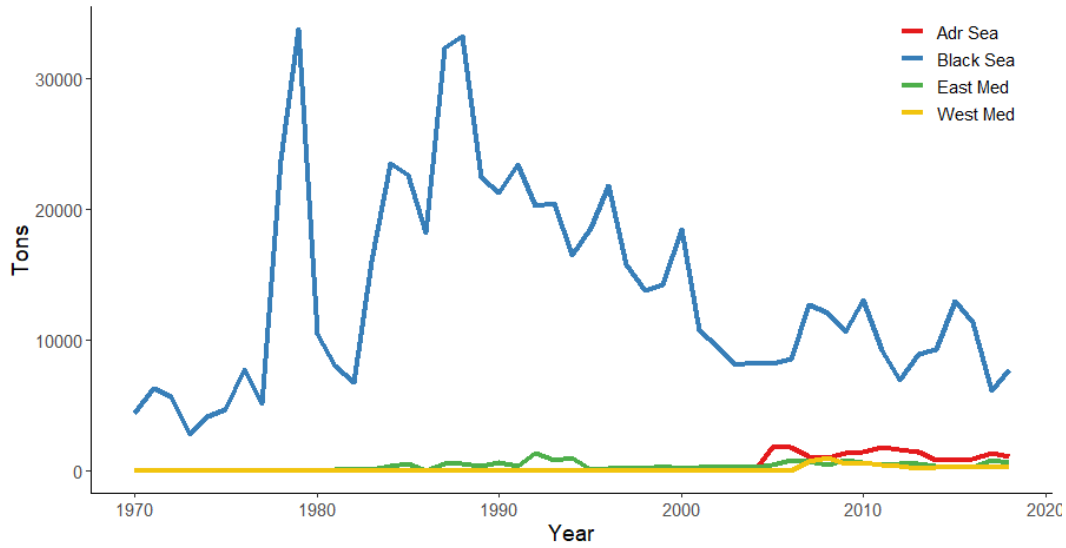

Figure 6. Landing data of the whiting (*M. merlangus*) from all the Mediterranean Sea, from 1970 to 2018. Source: FAO.

Looking at the northern Adriatic Sea, the Clodia database provides a long time series of landing data, collected from the official statistics of the fish market of Chioggia, whose fishing fleet is the major operating in the area, and one of the biggest of the Mediterranean Sea (Barausse *et al.*, 2009; Mazzoldi *et al.*, 2014). The database permits to evaluate the landing trend resulting from the activities of the local fleet, from 1945 to 2021.
In the case of whiting, it is to be noted a peak of catches in 1977, equal to 505.708 tons, followed by a rapid decrease. In the last thirty years, the landings seem rather constant, despite annual fluctuations (Figure 7).

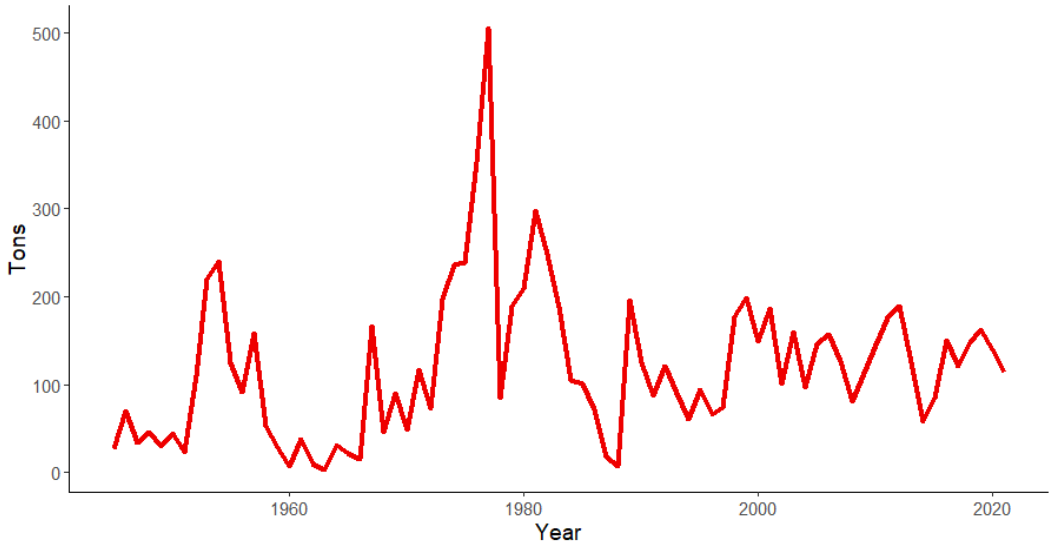

Figure 7. Landing data of the whiting (*M. merlangus*) from Chioggia Fish Market from 1945 to 2021. Source: Clodia database.

2. AIMS

The aim of this thesis is to study the population structure of *M. merlangus* in the northern Adriatic Sea, where this species is commercially exploited. Basing on a monthly sampling from fishing landings the study will provide: age estimations by otoliths reading, updated biological data, that will be used together with age data to estimate the growth rate in the study species.
Thanks to the availability of old otolith samples, these data will be used to perform a historical comparison of the population sampled in the year 2020-2021 with that sampled in 1990-1991, to investigate the presence of any differences in the structure that may have occurred over the span of thirty years.

3. MATERIALS AND METHODS

3.1 Study area

The Adriatic Sea is a semi-enclosed elongated basin of the Mediterranean Sea (Figure 8), surrounded by Italy on the west, Croatia and Slovenia on the east. Its main axis NW-SE has a length of 800 km and a mean width of 180 km. The morphological differences along both the longitudinal and the transversal axis of the basin allow its division into three sub-basins (Russo & Artegiani, 1996).

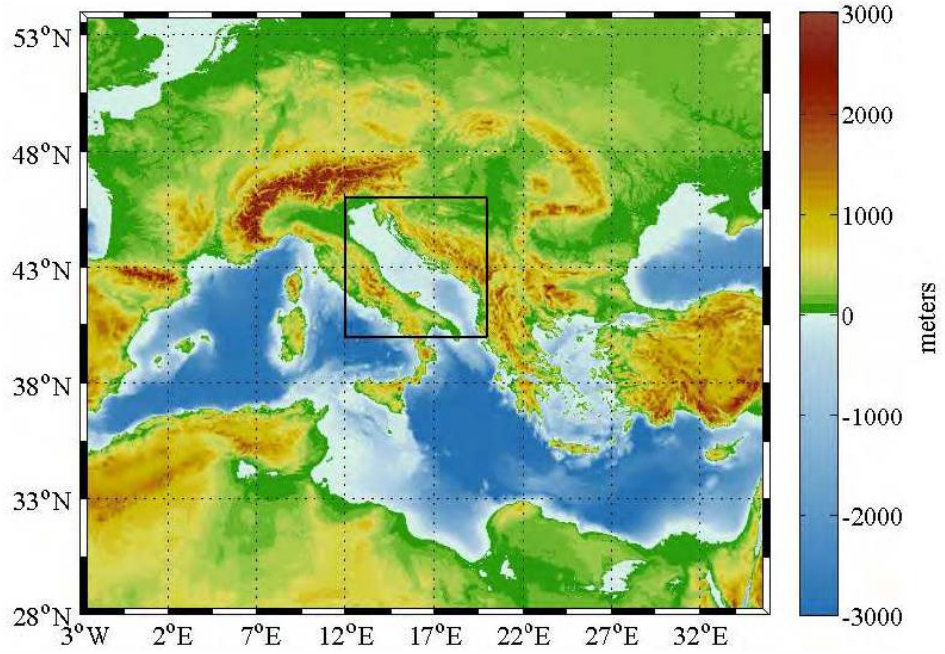

Figure 8. Orography and bathymetry of the Mediterranean region. The inset shows the Adriatic basin (Russo *et al*., 2012).

The northern sub-basin extents from the northernmost coast (NW) to the 100 m bathymetric line. It is characterized by a shallow mean depth of about 30 m and a very weak bathymetric gradient along the longitudinal axis. The Po and the other northern Italian rivers are responsible for a strong river runoff in this basin (~ 3000 m^3/s) and the source of about 20% of the total Mediterranean river runoff. The largest proportion of the river Po input in this basin flows south along the coast, but significant eastward freshwater fluxes are also present in all seasons, more markedly in winter. The coastal belt south of the Lagoon of Venice is the most eutrophic area, mainly due to river inputs, while oligotrophic conditions prevail along the eastern part of the basin (Solidoro *et al.*, 2009). The middle Adriatic is a transition zone between the northern and the southern sub-basins, extending from the 100 m bathymetric line to the Pelagosa sill. It is characterized by two depressions, the two Pomo (or Jabuka) Pits, reaching about 270 m as maximum

depth. The southern sub-basin extends to the Strait of Otranto. It reaches the greatest depth of all the three sub-basins, with a maximum depth of 1270 m (often referred to as the south Adriatic Pit). Both the western and eastern coasts have a narrow continental shelf and a steep continental slope. The western coast is generally sandy and quite regular, with a moderate slope; the eastern coast is irregular, characterized by many islands, and a rocky sharply sloping bathymetry (Russo & Artegiani, 1996).

The sediment grain-size composition is heterogeneous: sands and silty clays are prevalent, followed by silty sands and loams. Clayey sands and clays are scarcely present. It is possible to find fine sediments along the northern and the central Adriatic coastline of Italy, whereas sandy sediments occur along the Croatian coast. Intermediate compositions are present in between (De Lazzari *et al.*, 2004).

Some of the Adriatic water masses originated inside the basin and some others come from outside the basin. The Levantine Intermediate Water (LIW) are distinguishable by the intermediate salinity maximum in the water column. They originate in the Levantine basin and enter the Adriatic Sea through the Otranto Straits. Also entering in the Adriatic Sea through the Otranto Straits are the Ionian surface waters and a northward sub-branch of the Atlantic Surface Waters, entering the Mediterranean Sea through the Gibraltar Strait, then following the African coast. The ASW along its path is distinguishable by a subsurface salinity minimum.

The most important water masses originating in the Adriatic Sea are the bottom waters. A certain amount of the Adriatic bottom waters is formed in the northern sub-basin, the NAdDW (Northern Adriatic Deep Water), characterized by a very low temperature, relatively low salinity and high density. Superficially, a main current moves up along the eastern coast - Albania, Croatia - and then descends along the western Italian one. The flow along the western coast results from three gyres, one for each sub-basin, that only in autumn are connected with each other (Figure 9). The three sub-basins exhibit, with a certain seasonal variability, a cyclonic circulation (Russo & Artegiani, 1996).

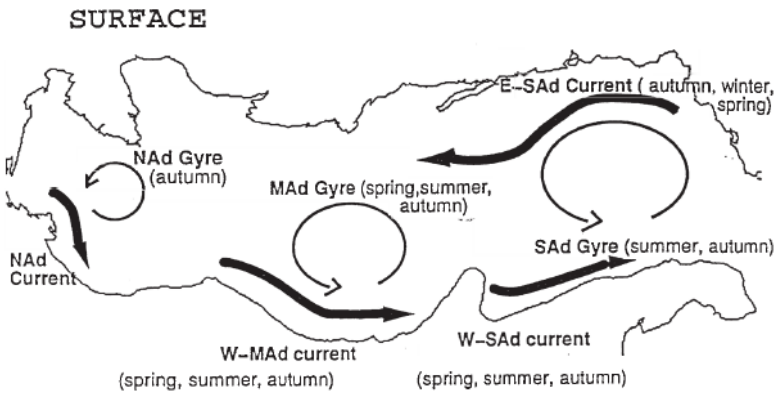

Figure 9. Surface water circulation in the Adriatic Sea (Russo & Artegiani, 1996).

The position of the northern Adriatic Sea and the shallowness of the bathymetry concur to characterize its peculiarity. Besides topographic features, atmospheric forcing, such as wind stress, heat fluxes and freshwater inputs from the main rivers along the Italian coast s are the main processes that define the physical properties and the dynamics of the northern Adriatic (Solidoro *et al.*, 2009).

Wind regime strongly influences the Adriatic Sea circulation, with significant differences between summer and winter. In summertime, besides local breezes, the dominant wind is the Maestrale, coming from the northwest. During winter season, the Scirocco, warm and humid, from the southeast, and the Bora wind, dry, cold and strong, from the north and the north-east, blow over the Adriatic Sea (Russo & Artegiani, 1996). Because of intense evaporation during winter, caused by these winds blowing over the northern Adriatic, dense water is formed (Artegiani *et al.*, 1989; Gačić *et al.*, 1999).

The Adriatic Sea has the greatest observed seasonal thermal gradient in the Mediterranean Sea, especially in the northern Adriatic, where near the coast the surface temperature ranges from about 5° C in winter to 27° C in summer. Variations are more limited offshore, with a range of 10-12° C. In winter, a thermal gradient at 5 m depth is pronounced along the longitudinal axis, while during summer this gradient is almost flat. This is due on one hand to the strong heat loss of the northern Adriatic during autumn-winter, and on the other hand to the extreme shallowness of the northern Adriatic sub-basin: it becomes extremely cold in winter because the vertical convection is limited by the shallow sea bottom, while in summer, despite the scarce heat fluxes, the temperature reaches high values, because the mixed layer is thin, due to the sub-basin shallowness, and the thermal stratification is enhanced by the hyaline one. During winter and autumn, especially in the northern and middle sub-basins, a transversal thermal gradient is also present, so that the waters near the western coast present a lower temperature than those of the eastern coast. During the summer period this gradient almost disappears (Russo & Artegiani, 1996).

Salinity variations are much pronounced near the western coast than offshore and are strongly influenced by Po and other northern rivers' outflow in the surface layer (Russo & Artegiani, 1996). An inverse gradient, from the Italian coast towards the middle of the basin, is instead detected in the case of nitrates, phosphates and silicates, whose presence is strictly related to the riverine inputs. The same gradient can be noticed for the chlorophyll, which shows the highest concentrations in the western coastal area in winter and in the southern coastal area in spring, with average values higher than 2 and 3 μg/l, respectively (Solidoro *et al.*, 2009).

3.2 Data collection

Two sampling activities were conducted to collect the samples used for this work, one approximately 30 years after the other.
The first one was carried out in the months of March, June, July, October, and November of 1990 and in the months of January, April, July, September, October and December of 1991. Fish samples were collected from trawling activities in the fishing area in front of the Po river mouth, by means of an Italian-type bottom otter trawler ("Tartana") aboard of the R/V "Salvatore Lo Bianco" of the Institute for Research on Maritime Fishing (CNR) of Ancona.
The second sampling activities were carried out monthly from November 2020 to December 2021. Samples were gathered by otter trawlers at landing sites, from fishing vessels that are part of the Chioggia's fleet, selecting the ones that usually fish in the area of interest to obtain a representative sample. Some specimens from long-line captures were added in order to increase the size range of the sampled population with the aim of obtaining an accurate evaluation of the maximum lifespan of the species. In fact, the specimens' size from this fishing gear is meanly bigger in comparison to those caught by trawled gears because of its higher selectivity. However, these specimens were not used for the comparison with the older samples, coming exclusively from trawling activity.
For each individual, the total length (TL) to the nearest millimeter was measured using a specific ruler and the weight to the nearest 0.1 g was determined using a precision balance (RADWAG PS 4500/C/1, d = 0.01 g). Sex and maturity stages were determined by macroscopic examination of the gonads using the MEDITS scale, proposed for gadid species (*Micromesistius potassou;* Follesa & Carbonara, 2019), once the specimens were dissected. Both left and right otoliths (*sagittae)* were extracted from each individual by making a cut along a frontal plane, starting from the front of the head above the eyes and continuing towards the back of the head, using a box cutter. Once exposed and identified, the otoliths were extracted with the help of a tweezer, cleaned with ethanol 70% and stored dry in test tubes in numbered vials.

3.3 Age estimation

From the whole fish sample, representative subsamples were selected for each sampling period, grouping specimens in 1 cm total length (TL) classes. The otoliths of max. 2 individuals per month per TL class were selected for the successive age determination and statistical analysis, to have a comparable sample in terms of sex, size and sampling period.

3.3.1 Otolith preparation

In order to highlight seasonal pattern of increments and make the age estimation easier and more accurate, the otoliths were burned and transversally sectioned (Tomas, 2006; Polat & Gümüs, 1996, Dufour *et al*., 2020, Polat & Gümüs, 1996). The peculiar conformation of the otoliths of this species, in fact, made the direct (on untreated otoliths) age estimation difficult, due to the thickness assumed by these structures as the deposition goes on, and the characteristic presence of bumps. Furthermore, a marked opacification of the samples was noted with storing time (Figure 10), so that the otoliths of the individuals sampled in 1990-91 were homogenously white and impossible to read from the outside.

Figure 10. Comparison between the same otolith after the extraction (*left*) and after six months (*right*). A marked opacification is visible.

Several attempts (immersion in alcohol, immersion in sea water, trasversal sectioning, longitudinal sectioning, and burning) were made in order to obtain samples that were as much readable as possible, especially with opacified ones. Finally, the burning and sectioning techniques were considered as the more appropriate and time-effective methods to use.
Selected otoliths were burned in a muffle (Prederi ME320), at 320° C x 4 mins. The left otolith was always chosen in order to standardize the procedure and, in case the left one was lacking or damaged, the right otolith was used.
Each previously burned otolith was fixed to a microscope slide with CrystalBond mounting adhesive and ground (Figure 11) with the planar grinding/polishing machine Remet LS2, with water-based abrasive paper (granulometry P400, P800 or P1200, according to the otoliths' size and brittleness) to form a base for the section. Once ground, the resin was heated again and the otolith moved vertically to the center, in such a way as to be able to smooth the opposite side and create the cross section to be read. To be sure to reach the best possible reading plane, where the *core* is clearly visible, the *sulcus acusticus* is deepened toward the *core* center and the rings are well distinguishable, the samples were progressively and gradually

ground and observed with a stereomicroscope under reflected light (Leica S6). Finally, each section was polished by means of a polishing cloth impregnated with Allumina powder 0.05 μ.

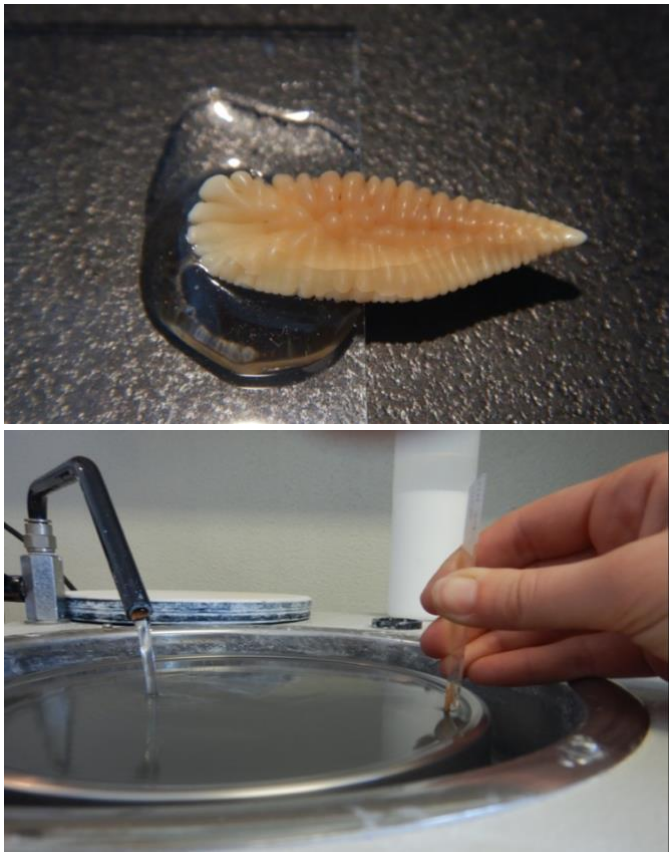

Figure 11. *Above*: otolith fixed through the resin to a microscope slide. *Below*: grinding procedure during the samples' preparation.

Samples were blindly read in random order, not knowing either the date of capture or the sex or the size of the specimen. Sections were observed and read using a stereomicroscope (Leica MZ6) using a magnification between 10-20x, immersed in water over a black surface under reflected light. A digital camera connected to the microscope together with an image analysis software (Leica Application Suite 4) was used for taking pictures of the samples and measuring the first *annulus*. The reading was performed by two operators twice, independently. The age was estimated as the number of completely formed *annuli* - one opaque and one translucent ring sequentially (Figure 12).

The age and the edge type (translucent or opaque) of each otolith sample were determined. For this work, the edges were considered as translucent/opaque in formation if the marginal increment was clear and distinguishable on the section margin. As for the age determination, also the marginal increment definition was carried out by two operators independently. In case of disagreement, the sample was not used for the validation. The edge condition (percentage of otoliths with

an opaque margin each month) was analysed in order to determine the periodicity and timing of ring formation. This method allowed the annual formation of the rings to be determined.

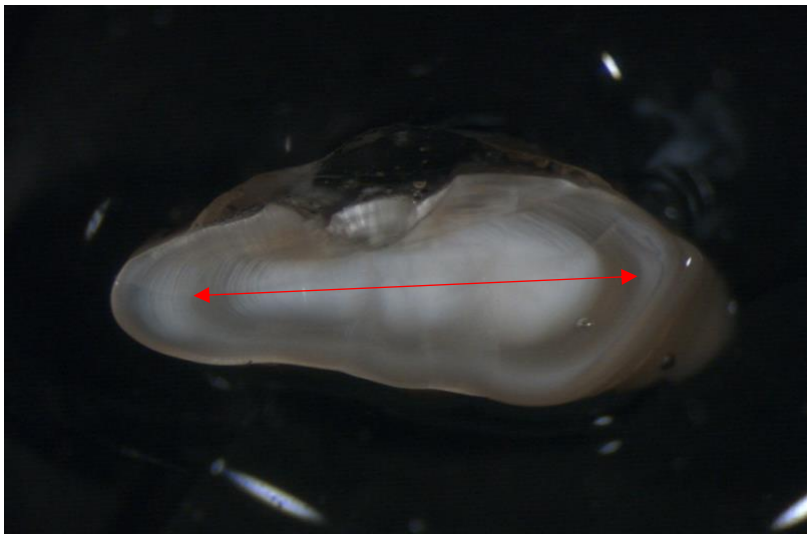

Figure 12. Example of burnt and sectioned otolith. In this photo is visible the first *annulus* completed (arrow). The marginal increment is translucent.

3.3.2 Age class assessment

In order to assign each specimen to one of the age groups, a single conventional date of birth for the entire population has been established. Given the low number of classes, the age was estimated in months, based on both the date of birth and the date of capture of the specimen. This also allowed a better fitting of the Von Bertalanffy growth model, and a more precise estimate of the growth rate.
The age estimation was therefore carried out according to the conventional date of birth, set on January 1, and established on the basis of the readings previously made and the nature of the marginal increments. The age, expressed in months, relative to the specimens with TL greater than 12 cm was assigned by dividing the year into quarters and considering both the age classes (0, 1, 2) and the margin (opaque, OP; translucent, TR) assigned. Age 0 and opaque edge were assigned to all the specimens smaller than 12 cm, as after several attempt of age estimation, it was seen that the smallest specimens had completely opaque otoliths. Thus, the size was used to infer the age so that they could undoubtedly be assigned to the first age class (age 0). Their age in months was always estimated as M-1.
The table below (Table 1) summarizes the age estimation method used. The quarters refer to the month of capture. So, a fish captured in February belongs to the Quarter 1, one caught in June to the Quarter 2, and so on.

AGE CLASS	EDGE	QUARTER 1	QUARTER 2	QUARTER 3	QUARTER 4
0+	**OP**	M-1	M-1	M-1	M-1
0+	**TR**	12 + (M-1)	12 + (M-1)	M-1	M-1
1+	**OP**	12 + (M-1)	12 + (M-1)	12 + (M-1)	12 + (M-1)
1+	**TR**	24 + (M-1)	24 + (M-1)	12 + (M-1)	12 + (M-1)
2+	**OP**	24 + (M-1)	24 + (M-1)	24 + (M-1)	24 + (M-1)
2+	**TR**	36 + (M-1)	36 + (M-1)	24 + (M-1)	24 + (M-1)

Table 1. Method of assigning the age in months for the three age groups recorded in the study population. 0, 1, 2 = estimated age. OP = opaque edge; TR = translucent edge; M = month of capture.

3.4 Data Analysis

Both the length-frequency distribution (LFD) and the edge-zone analysis were performed with R software. In order to estimate the accuracy of age estimation between the two operators, the Average Percentage Error (APE) and the Coefficient of Variation (CV) were computed as:

$$\text{APE} = 100 * \frac{1}{R} * \sum_{i=t}^{R} \frac{|Xij - \overline{Xj}|}{\overline{Xj}}$$

$$\text{CV} = 100 * \frac{\sqrt{\sum_{i=t}^{R} \frac{(Xij - \overline{Xj})^2}{R-1}}}{\overline{Xj}}$$

where *Xij* is the *i*th age determination of the *j*th fish, *Xj* is the mean age estimate of the *j*th fish, and *R* is the number of times each fished is aged (Panfili *et al.*, 2002). For each subsample the age-length keys were created using Microsoft Excel. Statistical analyses were performed using the Growth II software (PISCES Conservation Ltd, Lymington, UK). To describe the growth of the considered whiting sub-samples, the following Von Bertalanffy growth equation was implemented:

$$L_i = L\infty \, (1 - e^{-k(t-t0)})$$

where L_i is the length at age t_i, $L\infty$ is the maximum asymptotic length obtained from the individual average in the population, k is the growth coefficient (instantaneous growth rate), influencing the curvature of the function, and t_0 is the theoretical age when size is zero. In both females and males growth curves, created using R, the unsexed juveniles were included in order to improve the fitting of the model in the first period of growth. The differences between the growth models of the subsamples and the derived parameters were tested using the Kimura Likelihood-ratio test (Kimura, 1980), which allows to compare the values obtained in the growth models and determine their statistical significance.

4. RESULTS

4.1 Population structure

The total number of samples (N) selected for this analysis is 511 (180 males, 190 females, 141 unsexed) out of 1895 from 1990-91, and 480 (210 males, 243 females, 27 unsexed) out of 742 samples from 2020-21. The sex ratio (M/F) of the entire samples was equal to 0.93 in 1990-91 and to 0.83 in 2020-21, slightly biased towards females.

The Length-Frequency Distribution (LFD) of the sampled population, sorted by sex, is reported below (Figure 13). In the sample from 1990-91 (Figure 13a) the distribution is unimodal around 18 cm for both sexes, because male and female distributions mostly overlap, while in the 2020-21 curve (Figure 13b), the distribution is bimodal because the two distributions detach and the most abundant length classes are 16 cm for males, 22 cm for females. Furthermore, the maximum size (TL) is greater in the case of individuals fished between 1990-91 (males: 30 cm, females: 37 cm) compared to individuals from 2020-21 (males: 24 cm, females: 31 cm). Individuals below 12 cm in size were excluded from this analysis because in 1990-91 they were not sexed, probably due to the difficulties of sex determination in small and immature individuals. Even if some sexed juveniles (<12cm) from 2020-21 were present, they were not considered for this graph, to make the comparison fairer.

a.

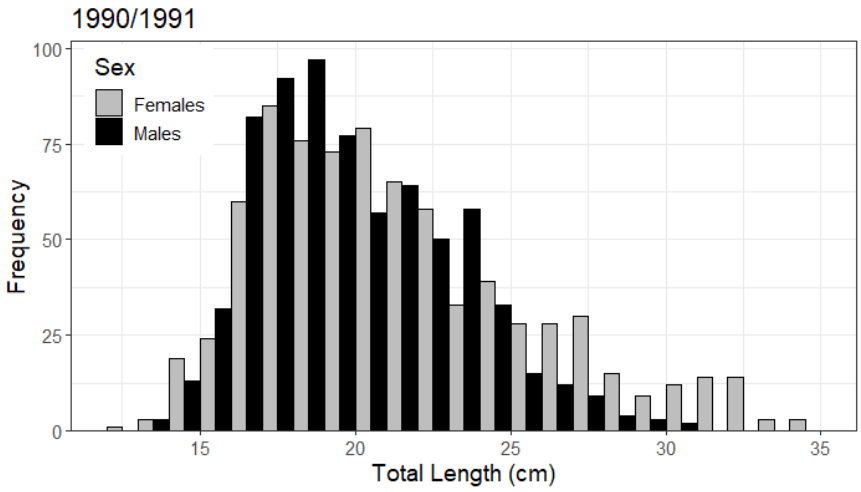

b.

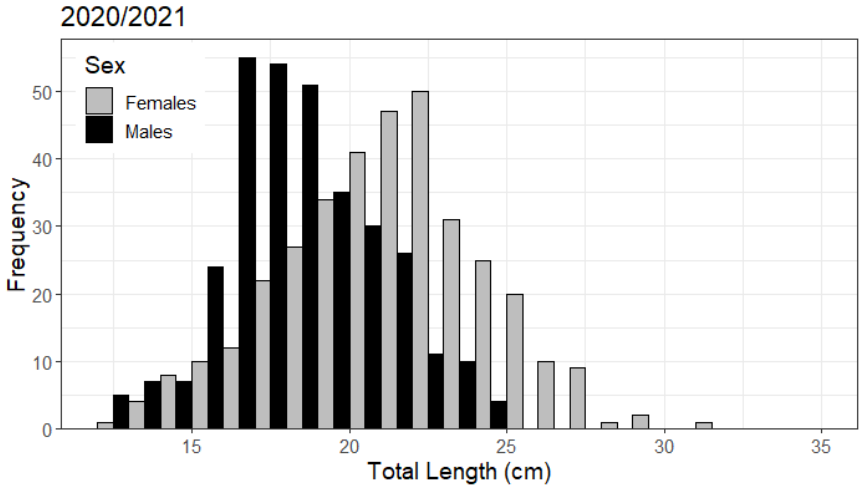

Figure 13. Length-Frequency Distribution (LFD) of the sampled population. a: samples from 1990-91. b: samples from 2020-21.

4.2 Ageing

As for the otoliths' readings, the edge-zone analysis showed an annual sinusoidal curve, which confirms that only one *annulus* is laid throughout the year. A slight difference in the width of the deposition timing of the opaque ring (Figure 14) was detected. The latter, in fact, seems to be wider in the past (a), roughly from April to September, with a higher percentage of samples showing the opaque edge-zone in September. In the case of the sample from 2020-21 (Figure 14b), the time-window in which most of the otoliths have an opaque edge narrows from May to the end of the summer, with a peak in July.

a.

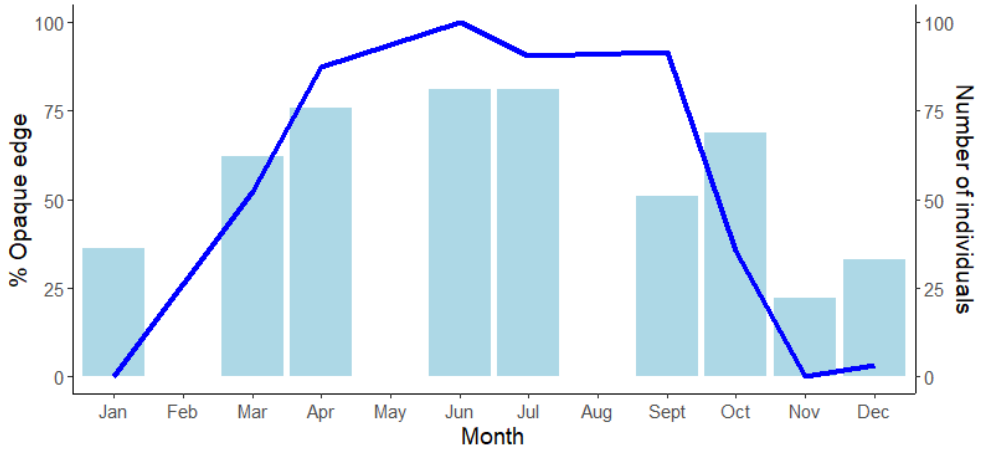

b.

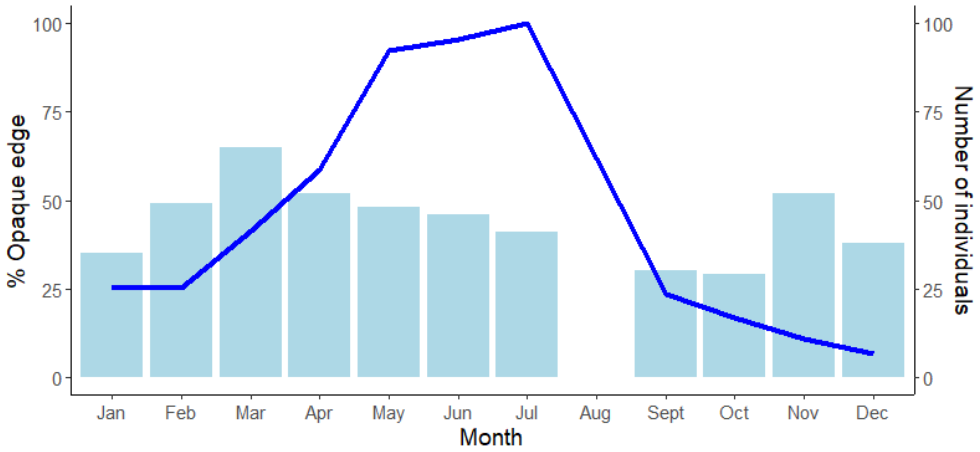

Figure 14. Timing of the opaque marginal increment of the whiting otoliths in a year. The graphs represent the percentage of samples in which an opaque edge-zone was recorded (dark blue line) and the number of individuals processed (light blue bars) (a: samples from 1990-91; b: samples from 2020-21).

After the otoliths' reading, the average percentage error (APE) and the coefficient of variation (CV), indices for age precision, were calculated between the ages estimated by the two operators. For the age estimation of the sample from 1990-91, the APE was equal to 1%, the CV equal to 1.4%. For the age estimation of the sample from 2020-21, the APE and the CV were 0.9% and 1.3%, respectively. For both samples' age estimation, the indices resulted very low, indicating high precision of readings.

The age classes obtained from otolith readings of the selected subsamples were only 3 (age 0, 1, 2). For this reason, to represent more clearly the age distribution of the population, age values were estimated in months rather than years. The age-length keys synthetize the population structure divided by TL and age classes. They allow understanding the relation between the age of the individuals and their size, so they are useful to evaluate the mean growth rate of individuals. In Figure 15 the age-length keys of the two whole subsamples are reported. In Annex A the keys for females (Annex A, Figure 19-20a), males (Annex A, Figure 19-20b), and unsexed juveniles (Annex A, Figure 19-20c) are reported. The year was divided into quarters to better visualize the population structure (January, February, March: Quarter 1; April, May, June: Quarter 2; and so on). In both subsamples, the greatest number of individuals has 15 months of age or less. While in 1990-91 the modal value is 6 months, in 2020-21 it is 15 months.
Also, it has to be noted that in 1990-91 at the same age, females reach bigger size than males (females 37 cm, males 30 cm, both 2 years old). The same size-based sexual dimorphism, but with smaller sizes in both sexes, is clearly visible in the

2020-21 subsample, in which the oldest male and female reach 22 cm and 29 cm respectively.

a.

ALL 90-91	QUARTER												
TL 1 cm	3	6	9	12	15	18	21	24	27	30	33	36	N
3	1												1
4	7												7
5	21												21
6	35												35
7	12												12
8	8												8
9	1	4											5
10	1	3											4
11		6											6
12		8	1										9
13		22	4										26
14		41	14										55
15		6	8	2									16
16		5	8	2									15
17		7	8	4									19
18		7	8	5	2								22
19		8	8	6	3								25
20		5	8	8	4								25
21		4	8	9	6	1							28
22		3	7	7	5	1							23
23		1	7	8	6	2		1					25
24			4	3	5	4	1	3					20
25		1	1	4	3	2	3	2	1				17
26			4	8	5		2	3	1				23
27			1	4	5	4	2	2	1				19
28			1	2	2	3	2				1		11
29				1		3	1	1			1		7
30				1	1	3	1	1		1			8
31					1	2	1	1					5
32						2	2	3		1			8
33						1	1						2
34						1	1						2
35							1						1
37									1				1
N	86	131	100	74	48	29	18	17	4	2	2	-	511

b.

ALL 20-21	QUARTER												
TL 1 cm	3	6	9	12	15	18	21	24	27	30	33	36	N
4	1												1
6	13												13
7	15	1											16
8	11	2											13
9	5	2											7
10	2	2											4
11		3											3
12		6											6
13		10			1								11
14		9	2	4	3								18
15		5	7	10	10	2							34
16		7	6	10	12	2							37
17		8	8	12	11	3							42
18		4	7	11	15	6							43
19		1	5	12	10	7							35
20			8	9	10	10	1	3	1				42
21			3	8	10	9	2	3	2	1			38
22			4	5	7	10	2	2	2	1		1	34
23			1	4	7	4	2	4	2				24
24				3	3	5		2	2				15
25				2	3	6	1	3	2				17
26					1	1		2	3	1			8
27						2		5	2			1	10
28						1		1				1	3
29								1				1	2
30						1		1		1			3
31								1					1
N	47	60	51	90	103	69	8	28	16	4	-	4	480

Figure 135. Age-length key of the whole 1990-91 (a) and 2020-21 (b) subsamples.

The values of the asymptotic length ($L\infty$), growth coefficient (k) and the theoretical age when fish size is 0 (t_0) estimated for the von Bertalanffy growth curve are reported in the table below (Table 2):

	$L\infty$	k	t_0	φ
1990-91 population	29.47	1.633	0.052	3.1517465
2020-21 population	22.84	1.889	-0.043	2.9936242
1990-91 females	35.14	1.219	0.045	3.1776072
2020-21 females	25.11	1.663	-0.04	3.0205857
1990-91 males	26.7	1.831	0.059	3.1157109
2020-21 males	20.52	2.236	-0.02	2.9738265

Table 2. Values of asymptotic length, k, t_0 and φ', estimated for the von Bertalanffy curve.

The curves here reported (Figure 16a and 16b) refer to the two entire subsamples, while the ones referring to females and males are reported in Annex B (1990-91: Figure 21a, b and 2020-21: Figure 22a, b).

a.

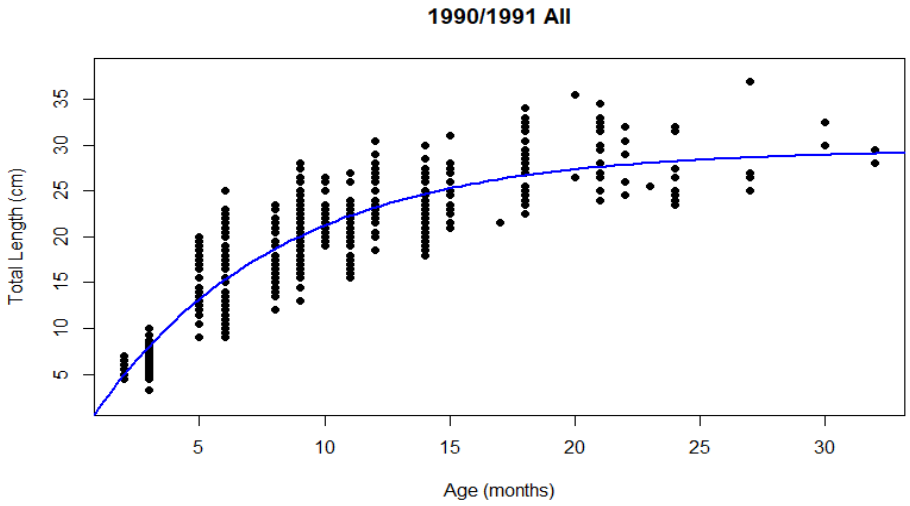

b.

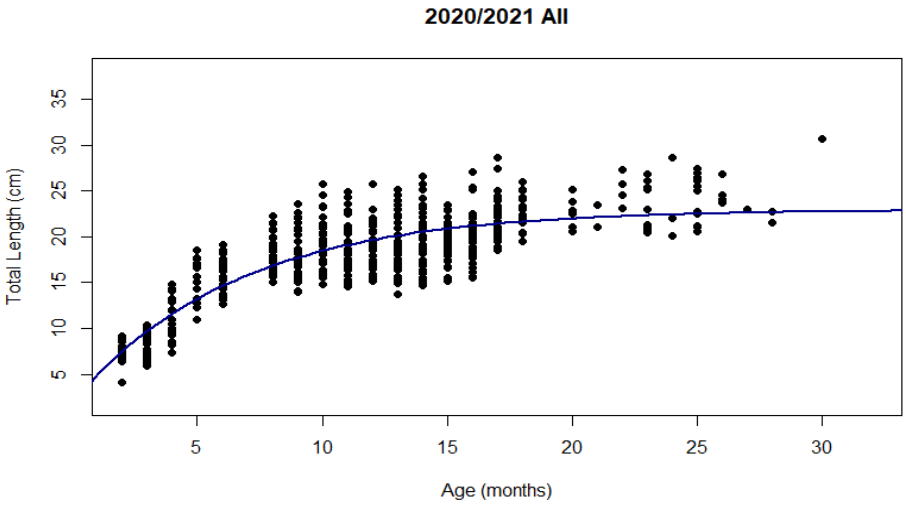

Figure 16. Von Bertalanffy curves for the whole 1990-91 (*above*) and 2020-21 (*below*) subsamples.

The Kimura test applied to Von Bertalanffy growth curves indicates that individuals sampled in 1990-91 reached larger sizes than those sampled in 2020-21, with $L\infty$ value significantly larger in the 1990-91 samples. This result is showed both in the comparison of the entire population in the two periods considered (χ^2=33.25, $p<0.01$) and in the comparison between males (χ^2=29.16, $p<0.01$) and between females (χ^2=28.64, $p<0.01$). Moreover, the k values comparison shows a statistically relevant difference (χ^2=13.2, $p<0.01$) between males and females from the 1990-91 sample. Even if increased compared to the past (Table 2), the k value of the most recently sampled population did not show a statistically significant difference when compared with the 1990-91 samples, nor in the comparison between males and females (Table 3). The value of t_0 so close to 0 indicates that the model fit to the data is good, even in the early stages of growth.

The phi-prime index calculated for the entire populations indicates that the growth performance slightly decreases compared to the past, and this is true also comparing singularly past and present females and past and present males.

		χ^2	p-value	Significance
Pop 90-91 vs Pop 20-21	L∞	33.25	<0.01	**
	k	1.1	0.29	ns
	all	255.78	<0.01	**
Fem 20-21 vs Mal 20-21	L∞	19.23	<0.01	**
	k	2.5	0.11	ns
	all	94.62	<0.01	**
Fem 90-91 vs Mal 90-91	L∞	42.39	<0.01	**
	k	13.21	<0.01	**
	all	80.07	<0.01	**
Fem 20-21 vs Fem 90-91	L∞	28.64	<0.01	**
	k	3.75	0.05	ns
	all	175.78	<0.01	**
Mal 20-21 vs Mal 90-91	L∞	29.16	<0.01	**
	k	1.45	0.23	ns
	all	177.69	<0.01	**

Table 3. Kimura test resulting values of chi-square and p-value for the asymptotic length (*L∞)*, growth coefficient (*k*) and the whole model (*all*); p<0.01.

Through the monthly sampling activities carried out in 2020-21, it was possible to identify the juveniles' cohort, following its growth during the early stages (Figure 17). Three months are reported below (April, May, and June 2021) to highlight the increasing size of the young-of-the-year, before they reach the same size as the adults, so they are not distinguishable anymore. The modal value of the length is 8 cm in April, 10.5 cm in May, 14 cm in June.

It was not possible to carry out the same analysis for the population sampled in 1990-91 due to the sample size of the considered months. The samples from April were very low in number, while there were no samples from May.

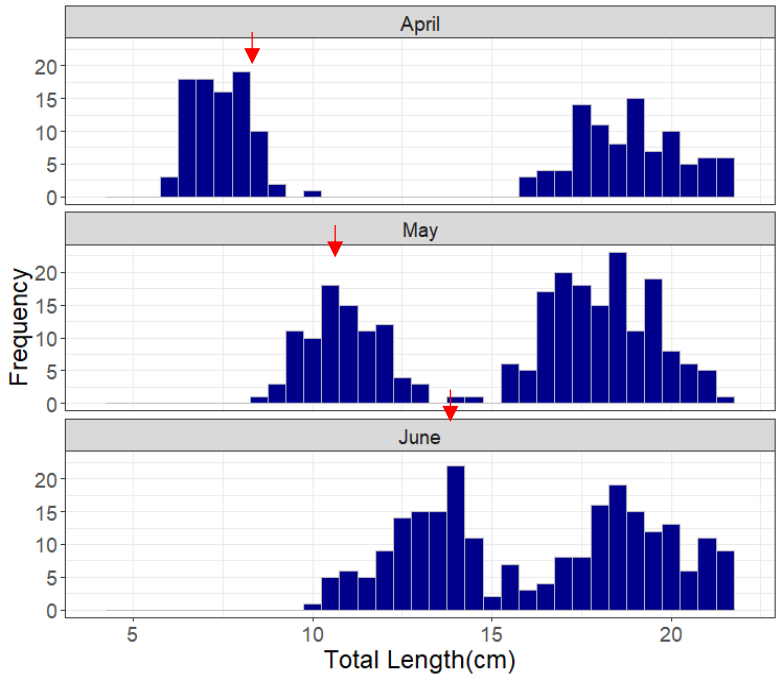

Figure 17. Monthly length-frequency distribution. The cohort of the young-of-the-year (2021) are clearly distinguishable.

5. DISCUSSION

In this work, the structure of the North Adriatic population of whiting was analyzed estimating the age classes by mean of otoliths' readings, defining the age-size relationship and building up the growth curve model. Furthermore, it was possible to make a comparison with the same population sampled in 1990-1991. Since whiting is a species of commercial interest for the north and central Adriatic Sea, and as there are few existing studies regarding this species in this area, the aspects concerning possible impacts of fishing pressure and/or environmental variations were - although not exhaustively - investigated.

Looking at the comparison between the two length-frequency distributions (LFD; TL 1 cm classes), divided by sex, a difference is appreciable in the maximum size sampled, that in both sexes is reduced compared to the past. As for the right tail of the distributions, the biggest sizes are reached by females, mirroring the known sexual dimorphism in size (Vallisneri *et al.*, 2004, 2006). In both cases, the higher number of individuals is gathered between 15 and 25 cm. Many fish species show sexual dimorphism in body size (Parker, 1992; Karin *et al.*, 2012; Kousteni *et al.,* 2019; Aydin *et al.*, 2011). Generally, somatic growth differences between males and females could result from several factors, often occurring simultaneously: dissimilarities in metabolic costs, different energy allocation patterns or unequal energy uptake levels between female and male specimens. The energy uptake level in turn could be influenced either by the quantity or the quality of the food ingested, or by different energy assimilation capacities. This means that, in the physiology or ecology of *M. merlangus*, there are differences between the sexes that favour higher growth performance in females. Moreover, in this species, different energy allocation patterns between sexes could result from the earlier onset of the sexual maturation of males (Lauerburg *et al.*, 2015), and in general a decrease in growth rate occurs in fish after attaining sexual maturation (Roff, 1983).

From the comparison between the two studied samples, a significant decrease in the asymptotic length (L_∞) emerged. Moreover, the growth coefficient (k), indicating the speed at which L_∞ is reached, showed a statistically relevant difference between males and females from the 1990-91 sample, mirroring the known intersexual growth difference. However, the most recently sampled population did not show the same difference in k values between males and females, even if a difference is present and it is reflected in the length-frequency distribution. Although not statistically significant, the k value of the 2020-21 population has increased compared to the past, in both males and females, and this, together with a significantly reduced $L\infty$ value, may indicate a slight trend towards a higher growth rate.

The asymptotic length may be decreased as a consequence of the fishing pressure exerted on this population. In fact, it is well-known that the largest sizes are those

most intensely removed from the population, which is therefore truncated and usually composed by fewer age classes and smaller individuals on average (Berkeley *et al.*, 2004; Hsieh *et al.*, 2010). These changes related to overexploitation occur when fishing pressure levels are so high to threaten fish stocks' maintenance. Indeed, one of the consequences of the strong fishing pressure is the decrease in the maximum size of the population, as a result of the constant removal of the larger and therefore older individuals. Also, the effects of this phenomenon are reflected in other important demographic aspects. For example, it is known the positive relationship between female size and fecundity (Ismen, 1995; Longhurst, 2002; Mehault, 2010). The latter can be drastically reduced due to the removal of larger females from the population and this can have unfavorable consequences on the reproductive capacity of the stock. As a consequence of size truncation, the reproductive output could be reduced (Murawski *et al.*, 2001), or there could be a reduction in sustainable yield (Heino & Godo, 2002). Several examples suggest that fishing-induced size truncation may lead to serious consequences for stocks' maintenance. For instance, this was likely to be the cause (or one of the causes) of the collapse of the Atlantic cod stock off Newfoundland (Olsen *et al.*, 2004, 2005), as well as the recruitment failure of the Arcto-Norwegian cod stock (Ottersen *et al.*, 2006), the declined lifetime egg production for rockfishes (O'Farrell & Botsford 2006a, 2006b), and the reduced reproductive output of several marine fishes (Venturelli *et al.*, 2009). However, even in these empirical studies it is difficult to separate fishing impacts from environmental effects (Hsieh *et al.*, 2010).

Therefore, another plausible explanation to be considered for the decrease of the asymptotic length and for the difference in the growth rate is represented by variations of environmental conditions. In this regard, interesting data comes from a case study in the North Sea, in which a sample of whiting was taken in 2007 and subsequently another in 2012. Sexual dimorphism (in terms of $L\infty$), stomach contents and growth rate were investigated and then compared. In 2007, the whiting showed 4 cm (females) and 2 cm (males) smaller $L\infty$ compared with 2012. These differences between the samples of the two years were less evident in juveniles and mainly resulted in fish larger than 25 cm TL. There was not, however, an appreciable decrease in the condition (in terms of body mass at age) of *M. merlangus* in 2007 compared with 2012. So, in this case, it is assumed that the observed discrepancies, to some extent, resulted from differences in the availability of prey fish in those two years in the North Sea. This is because *M. merlangus* during prolonged periods with low food availability might respond with reduced growth rates (Lauerburg *et al.*, 2015). In other words, variations in preys' or predators' abundance could influence periodically the biomass of the whiting. This aspect must be considered in the investigation regarding the causes of the different asymptotic lengths of the samples obtained in the present study.

Moreover, it is worth considering the hypothesis that the differences found at the level of asymptotic length could be attributed to cyclical population fluctuations, linked to the water warming trend consequent to the climate changes. In particular, *M. merlangus* is a typically cold-water species, therefore it must be considered, on one hand, its ideal temperature-related physiological range and, on the other hand, how climate change is increasing the sea temperature, and how this can affect the metabolism of marine species (Forster *et al.,* 2012). Unfavorable conditions can act as factors that lead the species towards modifications of life-history traits as adaptations. More likely, the observed changes in the population might be the result of the combination of all these factors.

Another significant feature to underline is that, in the data collected from the literature, there is a substantial difference in several life-history traits of the different whiting populations. The differences seem to be linked to the geographical distribution, therefore to the latitude or to the environmental characteristics of the areas inhabited by this species and are evident mostly between the Adriatic and the other basins that are part of the whiting distribution area. The Adriatic Sea seems to represent an exception compared to the other basins considered here, probably for the difference in the mean temperature that characterizes the waters of the North Sea and the adjacent basins. Moreover, the bathymetry, the trophic levels composition, the amount of nutrients deriving from the rivers' runoff, make the Adriatic ecosystem unique. Compared to the rest of the Mediterranean Sea, the northern Adriatic has the greatest quantity of phytoplankton biomass and it is consequently one of the most productive basins. A terrigenous supply of nutrients in some semi-enclosed bays and channels of the Croatian coast and all along the Italian coast via run-off, influences productivity in the north Adriatic coastal belt (Fonda Umani, 1996). The presence of these nutrients of riverine origin is strictly related to the path of the currents and masses of water that move from the mouth of the Po River towards the open sea, creating a gradient from the northwest coast to the south-southeast (Solidoro *et al*., 2009). The greater availability of food and energy in the ecosystem might lead several species that inhabit the northern Adriatic Sea to grow faster, compared to populations that inhabit oligotrophic waters.

In the case of whiting populations living at higher latitudes, such as those of the North Sea and the Irish Sea, adult specimens can reach 40-50 cm TL at around 5-7 years of age (Lauerburg *et al.,* 2015; Gerritsen *et al*., 2003); in the Baltic Sea, there are specimens up to 58 cm TL and 13 age groups (Ross *et al.,* 2018). In the case of the Black Sea population, however, the specimens reach smaller sizes in the same period, growing up to around 25 cm TL at about 6 years of age (Mazlum & Bilgin, 2014). In the Adriatic Sea, on the other hand, the growth rate seems to be much higher: although the number of age groups is very low, the sizes reached are equal to those recorded in adult subjects from other populations. In this basin, in fact, it seems that the specimens are able to grow on average up to 20 cm TL after the first

year of life (19.4 cm males, 21.5 cm females), and that they reach on average about 25 cm TL (23.1 cm males, 26.9 cm females) at the end of the second year of life (Giovanardi & Rizzoli, 1984). These data are confirmed by the present thesis work, in which the recorded female specimens presented a size greater than 35 cm at the end of the third year of life.
Below is reported a summary table of some important life-history traits relating to the different whiting populations studied so far and on which there are data in the literature, to summarize the main differences (Table 4). Size-based sexual dimorphism is typical of all the considered populations.

Area	Sex	TL_{max} (cm)	L_{mat} (cm)	Spawning peak	Age groups	References
Adriatic Sea	♂	28	16.1	December	3 (0-2)	Vallisneri *et al.*, 2006; Calì, unpublished data
	♀	33	16.8			
Black Sea	♂	20.4	13.9	February, April, November	7 (0-6)	Mazlum & Bilgin, 2014; Bilgin *et al.*, 2012
	♀	30.7	14.6			
North Sea	♂	35.7	19.3	April	8 (0-7)	Lauerburg *et al.*, 2015
	♀	40.8	22			
Irish Sea	♂	33.4	22	March, April	8 (0-7)	Gerritsen *et al.*, 2003
	♀	50.2	19			

Table 4. Available data about maximum total length (TL_{max}), length at maturity (L_{mat}), spawning peak and age classes in different geographical areas, divided by sexes.

As it can be seen, compared to the others, the population of the Adriatic Sea has a much smaller number of age groups, although reaching similar or only slightly lower sizes than those of the other seas considered in a shorter period of time. Moreover, the maximum size measured in 1990-91 was 37 cm for females and 30.5 for males, both aged as two years old. In the 2020-21 sample, the maximum size was 35.8 cm for females and 24.8 cm for males, also in this case both aged as two years old. These data highlight a difference in the growth of this population, which is undoubtedly faster, with a reduced maximum size compared to basins outside the Mediterranean Sea. Additionally, the computed phi-prime results higher for the Adriatic population compared to both that of the whiting population from the Black Sea (Yildiz & Karakulak, 2018) and to that of other Gadidae, as the poor cod (*Trisopterus capelanus*; Koç *et al.*, 2021). This indicates the higher growth performance of the whiting residing in the northern Adriatic Sea.
The differences in growth and the greater number of age classes in the populations other than the Adriatic one are also clearly identifiable in the otoliths. Below are showed the images of otoliths of individuals of the same length, one from the Adriatic Sea and the other taken from North Sea samples, which, by way of

example, highlight these inequalities. Beyond the evident difference in age, it is to be noted the differences regarding the shape of the otolith itself, which in this specific population appears to have an even more pronounced lanceolate shape and a reduced presence of the typical bumps (Figure 18).

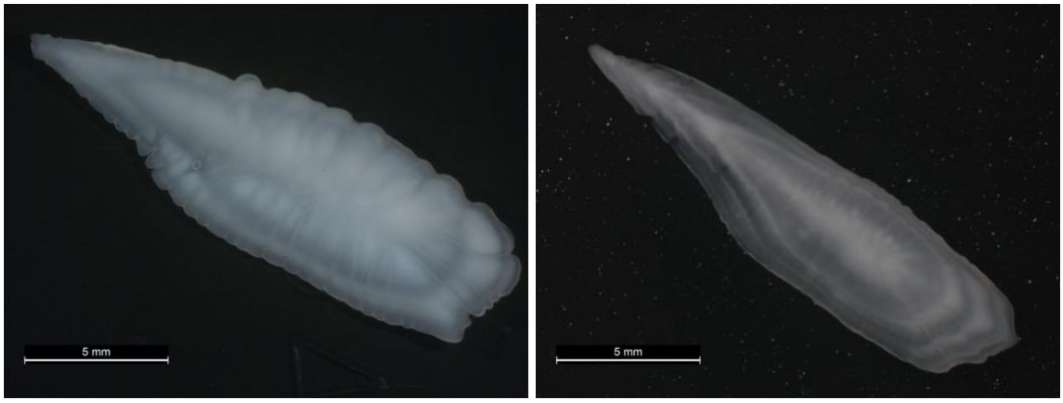

Figure 148. Comparison between northern Adriatic Sea (*left*) and North Sea (*right*) whiting otoliths. North Sea specimens came from landings in Chioggia wholesale fishmarket.

The case of whiting is not the only one in which a species inhabiting both the northern Adriatic Sea and basins at higher latitudes, shows an inter-population difference in the growth rate and that the latter is higher precisely in this Mediterranean basin. An example is represented by the north Adriatic population of turbot (*Psetta maxima*, L. 1758). The latter was compared with those of the North Sea and the Baltic Sea in the study by Arneri *et al.*, 2001. In the Adriatic Sea, the growth rate is slightly higher than in the North Sea (Mengi, 1963; Jones, 1974) and considerably higher than in the Baltic Sea (Szlakowski, 1990) and in the north-western Mediterranean Sea (Robert & Vianet, 1988). Adriatic turbot appears to belong to the population group with the fastest growth rates. Another example is represented by black goby (*Gobius niger*), which, in the Adriatic Sea, has a higher growth rate and attains a bigger size (Fabi & Giannetti, 1985) than in the West Coast of Ireland (King *et al.*, 1980) and in the Veerse Meer of Holland (Vaas *et al.*, 1975). It is known in the literature that warming increases growth and development rates, reducing maximum or adult size at the same time (Lindmark *et al.*, 2022). This can happen between different species but also between populations of the same species living at different latitudes, as in the case of the whiting. Therefore, it is worth considering that the differences in some life-history traits, both inter-population and inter-annual of the same population, could be attributable to the different anthropogenic pressures, that is to the fishing pressure exerted by human on stocks, as well as to ecological-environmental variations, in terms of temperature and/or availability of prey and the consequent adaptive strategies of the species to different external inputs.

On the other hand, variations in terms of prey availability could be a direct consequence of changes in the ecological structure of the Adriatic basin. The latter has been influenced in recent years by a trend towards oligotrophy in the northern Adriatic Sea (Penezić, 2022), also due to various factors, including mainly the decrease of the Po River rich-in-nutrients freshwater inputs (Gašparović, 2012).
The difference in the life-history traits among the different populations and above all the differentiation of some traits particularly in the Adriatic population compared to the others, however, raises the question of a possible genetic differentiation. Given the distance and the geographical separation between the Adriatic Sea and the northeast Atlantic, the connectivity between these populations after settling in the different areas may have been scarce, if at all, and the different environmental conditions may have influenced this divergence. The hypothesis of the presence of two different subspecies of *Merlangius merlangus* had already been advanced, with the Atlantic subspecies, *M. merlangus merlangus*, and the subspecies *Merlangius merlangus euxinus* typical of the populations of the Black Sea, Marmara Sea, and Azov Sea. The Adriatic population was believed to consist of both subspecies (Miliić & Kraljević, 2011). The temporal pattern of divergence between the two presumed subspecies is related to the Last Glacial Maximum (219 Kya), whereas the expansion of the Black Sea and the Turkish Straits System occurred after the flooding of the Black Sea by salt water from the Mediterranean (5 Kya), following a period of stability (Şalcıoğlu *et al.*, 2020). In the literature, we can find some investigations concerning the possible genetic variation of the Atlantic and Mediterranean populations. As far as the Mediterranean is concerned, however, no such investigation has been carried out in the Adriatic. Instead, the populations of the Black Sea, the Marmara Sea and the North Aegean Sea were considered. No clear distinction between the two presumed subspecies was detected. The lower genetic variability of the eastern Mediterranean *M. merlangus,* when compared to the Atlantic ones, might be due to a potential population bottleneck before the last glacial period, a trend that is commonly found in these waters (Şalcıoğlu *et al.*, 2020). A significantly heterogenic level of genetic structuring of whiting has been recorded within the North Sea. It appears that the North Sea is composed of at least three distinct population units (Southern Bight, Flamborough Head and a third unit grouping the Dogger Bank and the southern Norwegian coast), while the Celtic Sea to the western Hebrides encompasses a single metapopulation. In this second case, the genetic homogeneity may result, at least in part, from the widespread dispersal of the young pelagic stages through passive drift with the current systems (Charrier *et al.*, 2007). Spatial genetic analysis reveals genetic uniformity across long geographic distances suggesting a high level of gene flow (Eiríksson & Árnason, 2014).
Given the geographic conformation of the Adriatic basin and the scarcity of information in the literature regarding the whiting's population genetics in this area,

further investigations in this regard are deemed necessary. This need is supported by some evidence detected in several species present in the Mediterranean Sea. It has been observed a genetic differentiation between the northern-central Adriatic population e the southern one in the Atlantic mackerel (*Scomber scombrus*, Papetti *et al.*, 2019), as well as in the European anchovy (*Engraulis encrasicolus*, Bembo *et al.*, 1996; Borsa, 2002). The reason of these differentiations could be ascribed to physical barriers to migrations and/or to larval dispersal, among which the presence of a stable gyre dividing the northern and southern Adriatic waters (Russo & Artegiani, 1996), a bathymetric incoherence corresponding to the deep Jabuka (Pomo) Pits, and the strong spatial and temporal variability of trophic conditions in the northern – central Adriatic (Fonda Umani *et al.*, 1992). Additional analysis of population genetics and structure of the whiting would help to better define the boundaries of the different populations of this species and would be of great support in the definition of fisheries management policies in this area of the Mediterranean Sea.

6. CONCLUSION

This work aimed to analyze the population structure of the *Merlangius merlangus* species, to understand if external pressures, both human and environmental, may have caused changes that require attention. A significant difference was highlighted in the asymptotic length of the individuals that make up the population, therefore it was observed a reduction in the maximum sizes reachable by both males and females, beyond the known size-based sexual dimorphism. The stock is likely undergoing fishing pressure or environmental changes: it is a coldwater species in a sea that is warming and in which, additionally, a high fishing pressure is exerted. An exhaustive study of this population is necessary as very little is present in the literature about whiting in the northern Adriatic basin, although it is a highly exploited area, in which this species is fished for commercial purposes.

The reduction of the maximum size of this population can have serious consequences on the population structure, affecting the size of maturity, the fecundity and the renewal capacity of the stock. Studies like this can form the basis for proper stock management and appropriate fisheries regulation.

On the other hand, climate change and the constant increase in both atmospheric and sea temperatures are threatening these populations on another front. This species adapted to cold waters (Maximov *et al.*, 2011) and subsequently settled in some areas of the Mediterranean Sea could suffer the effects of this overheating in the long term. In addition to this, strong interactions exist between the effects of fishing pressure and the effects of climate. Fishing reduces the age, size, and geographic distribution and diversity of populations, besides the biodiversity of

marine ecosystems, making both more sensitive to additional stresses such as climate change (Brander, 2007).

Further studies would be necessary, in order to investigate the population genetics of this species in the Adriatic Sea and to evaluate its vulnerability. Differences in meristic and morphometric characters between whiting populations in the Atlantic Ocean, Black Sea and the Adriatic have been detected. These could be the result of spatial segregation and/or exposure to different environmental conditions. Further research is required to determine whether a subspecies of whiting exists and what is its status, as well as its real area of distribution. Finally, the phylogeny of this species should be investigated through genetic analysis techniques, which are less prone to subjective interpretation (Miliić & Kraljević, 2011).

BIBLIOGRAPHY

Arneri, E., Colella, S., & Giannetti, G., 2001. Age determination and growth of turbot and brill in the Adriatic Sea: reversal of the seasonal pattern of otolith zone formation. *Journal of Applied Ichthyology*, *17*(6), 256-261.

Artegiani, A., Azzolini, R., & Salusti, E., 1989. On the dense water in the Adriatic Sea, *Oceanologica Acta*, 12, 151–160.

Aydin, I., Sahin, T., Kolotoglu, L., & Özongun, M., 2011. The effect of sexual dimorphism on growth of the black sea turbot, Psetta maxima. *Journal of Fisheries Sciences.com*, *5*(1), 47

Barausse, A., Duci, A., Mazzoldi, C., Artioli, Y. & Palmeri, L., 2009. Trophic network model of the Northern Adriatic Sea: analysis of an exploited and eutrophic ecosystem. *Estuarine, Coastal and Shelf Science,* 83, 577–590.

Bembo, D. G., Carvalho, G. R., Cingolani, N., Arneri, E., Giannetti, G., & Pitcher, T. J., 1996. Allozymic and morphometric evidence for two stocks of the European anchovy *Engraulis encrasicolus* in Adriatic waters. *Marine Biology*, 126, 529–538.

Berkeley, A. S., Chapman, C. & Sogard, S. M., 2004a. Maternal age as a determinant of larval growth and survival in a marine fish, *Sebastes melanops*. *Ecology,* 85(5), 1258–1264.

Berkeley, A. S., Hixon, M. A., Larson, R. J. & Love, M. S., 2004. Fisheries Sustainability via Protection of Age Structure and Spatial Distribution of Fish Populations. *Fisheries*, 29:8, 23-32.

Bilgin, S., Bal, H. & Taşçı, B., 2012. Length based growth estimates and reproduction biology of whiting, *Merlangius merlangus euxinus* (Nordman, 1840) in the southeast Black Sea. *Turkish Journal of Fisheries and Aquatic Sciences*, 12(4), 871-881.

Bombace, G. & Lucchetti, A., 2011. Elementi di biologia della pesca. Edagricole, Bologna, 383 pp.

Bolognini, L., Domenichetti, F., Grati, F., Polidori, P., Scarcella, G. & Fabi G., 2013. Weight-length relationships for 20 fish species in the Adriatic Sea. *Turkish Journal of Fisheries and Aquatic Sciences*, 13(3).

Borsa, P., 2002. Allozyme, mitochondrial-DNA, and morphometric variability indicate cryptic species of anchovy (*Engraulis encrasicolus*). *Biological Journal of the Linnean Society*, 75, 261–269.

Brander, K. M., 2007. Global fish production and climate change. *Proceedings of the national academy of sciences*, *104*(50), 19709-19714.

Caddy, J. F., Refk, R. & Do-Chi, T., 1995. Productivity estimates for the Mediterranean: evidence of accelerating ecological change. *Ocean and Coastal Management,* 26, 1–18.

Campana, S. E., 2001. Accuracy, precision and quality control in age determination, including a review of the use and abuse of age validation methods. *Journal of fish biology*, *59*(2), 197-242.

Charrier, G., Coombs, S. H., McQuinn, I. H. & Laroche, J., 2007. Genetic structure of whiting *Merlangius merlangus* in the northeast Atlantic and adjacent waters. *Marine Ecology Progress Series*, *330*, 201-211.

Cohen, D. M., Inada, T., Iwamoto, T. & Scialabba, N., 1990. FAO species catalogue. Vol. 10. Gadiform fishes of the world (Order Gadiformes). An annotated and illustrated catalogue of cods, hakes, grenadiers and other gadiform fishes known to date. *FAO Fisheries Synopsis, 125(10*). Rome: FAO. 442 p.

Coll M., Piroddi C., Steenbeek J., Kaschner K., Ben Rais Lasram F., *et al.,* 2010. The Biodiversity of the Mediterranean Sea: Estimates, Patterns, and Threats. *PLoS ONE,* 5(8), e11842.

Colloca, F., Scarcella, G. & Libralato, S., 2017. Recent trends and impacts of fisheries exploitation on Mediterranean stocks and ecosystems. *Frontiers in Marine Science*, 4, 244.

Cooper, A. B., 2006. *A Guide to Fisheries Stock Assessment from Data to Recommendations. University of New Hampshire*. 44 pp.

Cooper, A., 1983. The reproductive biology of poor-cod, *Trisoptems minutus* L., whiting, *Merlangius merlangus* L., and Norway pout, *Trisoptems esmarkii* Nilsson, off the west coast of Scotland. *Journal of Fish Biology,* 22, 317-334.

De Lazzari, A., Rampazzo, G., & Pavoni, B., 2004. Geochemistry of sediments in the Northern and Central Adriatic Sea. *Estuarine, Coastal and Shelf Science. 59*, pp. 429–440.

Dufour, J-L., Chantre, C., Elleboode, R., Mahe, K., 2020. Estimation de l'âge du merlan (*Merlangius merlangus*). Rapport scientifique IFREMER, 54p.

Eiríksson, G.M. & Árnason, E., 2014. Mitochondrial DNA sequence variation in whiting *Merlangius merlangus* in the Northeast Atlantic. *Environmental Biology of Fishes*, 97**,** 103–110.

Fabi, G. & Giannetti, G., 1985. Growth parameters of the black goby (*Gobius niger* L.) in the Adriatic Sea, based on otoliths reading. *Rapport Commission International Mer Meéditerranée*, *29*(8), 87-90.

FAO. 2020. The State of World Fisheries and Aquaculture 2020. *Sustainability in action.* Rome.

Fiorentini, L., Caddy, J. F. & de Leiva, J. I., 1997. Long and short-term trends of Mediterranean fishery resources. *General Fisheries Council for the Mediterranean*. No. 69. Rome: FAO.

Follesa, M. C. & Carbonara, P., eds. 2019. *Atlas of the maturity stages of Mediterranean fishery resources*. Studies and Reviews n. 99. Rome, FAO. 268 pp.

Fonda Umani, S., 1996. Pelagic production and biomass in the Adriatic Sea. *Scientia Marina*, 60, 6-77.

Fonda Umani, S., Franco, P., Ghirardelli, E., & Malej, A. 1992. Outline of oceanography and the plankton of the Adriatic Sea. In *Marine Eutrophication and Population Dynamics*. Proceedings of 25th European Marine Biology Symposium, pp. 347–365. Ed. by G. Colombo, I. Ferrari, V. U. Ceccherelli, and R. Rossi. Olsen and Olsen, Fredensborg, Denmark. 395 pp.

Forster, J., Hirst, A. G., & Atkinson, D., 2012. Warming-induced reductions in body size are greater in aquatic than terrestrial species. *Proceedings of the National Academy of Sciences*, *109* (47), 19310-19314.

Gačić, M., Scarazzato, P., Artegiani, A., & Russo, A., 1999. Longterm variations of deep-water properties in the Middle Adriatic Pit. *The Adriatic Sea. Ecosystem Research Report*, *32*, 25-37.

Gašparović, B., 2012. Decreased production of surface-active organic substances as a consequence of the oligotrophication in the northern Adriatic Sea. *Estuarine, Coastal and Shelf Science,* 115, 33–39.

Gertwagen, R., Raicevich, S., Fortibuoni, T. & Giovanardi, O., 2008. *Il Mare Com'era*. Proceedings of the II HMAP Mediterranean and the Black Sea project; Chioggia (Italy), 27th-29th September 2006.

Giovanardi O., Rizzoli M., 1984. Biological data, collected during expeditions Pipeta, on the whiting, *Merlangius merlangius* (L.) in the Adriatic Sea. *FAO, Fisheries Report, 290*: 149-153.

Goldman, K. J., 2005. Age and growth of elasmobranch fishes. Management techniques for elasmobranch fisheries. In *Management Techniques for Elasmobranch Fisheries* (Musick, J. A. & Bonfil, R., eds), pp. 76–102. *FAO Fisheries Technical Paper* 474.

Haddon, M., 2011. *Modelling and Quantitative Methods in Fisheries*. 2nd edition. Publisher Chapman and Hall, CRC Press. 471 pp.

Hsieh, Ch., Yamauchi, A., Nakazawa, T. & Wang, W., 2010. Fishing effects on age and spatial structures undermine population stability of fishes. *Aquatic Sciences,* 72, 165–178.

Ismen, A., 1995. Fecundity of whiting, *Merlangius merlangus euxinus* (L.) on the Turkish Black Sea coast. *Fisheries Research*, 22 (3-4), 309-318.

Jackson J. B. C., Kirby M. X., Berger W. H., Bjorndal K. A. *et al.*, 2001. Historical overfishing and the recent collapse of coastal ecosystems. *Science*, 293, 629-638.

Jennings, S., Reynolds, J. D., & Mills, S. C., 1998. Life-history correlates of responses to fisheries exploitation. *Proceedings of the Royal Society of London. Series B: Biological Sciences*, *265* (1393), 333-339.

Jones, A., 1974. Sexual maturity, fecundity, and growth of the turbot *Scophthalmus maximus*, L. J*ournal of the Marine Biological Association of the United Kingdom,* 54, 109 ± 205.

Hüssy, K., Coad, J. O., Farrell, E. D., Clausen, L. W. & Clarke, M. W., 2012. Sexual dimorphism in size, age, maturation, and growth characteristics of boarfish (*Capros*

aper) in the Northeast Atlantic, *ICES Journal of Marine Science*, 69 (10), 1729–1735.

Kimura, D. K., 1980. Likelihood methods for the von Bertalanffy growth curve. *Fishery bulletin*, 77(4), 765-776.

King, P. A., Fives, J. M., & Dunne, J., 1980. Littoral and Benthic Investigations on the West Coast of Ireland: XII. The Fishes of Kylesalia Creek, Connemara. *Proceedings of the Royal Irish Academy. Section B: Biological, Geological, and Chemical Science,* 165-177.

Koç, H. T., Erdoğan, Z., & Burkay, H., 2021. Growth and reproduction properties of the poor cod, *Trisopterus capelanus* (Lacepède, 1800) (Gadidae) in the Edremit Bay, Northern Aegean Sea, Turkey. *Acta Biologica Turcica*, 34 (3), 114-121.

Kousteni, V., Anastasopoulou, A. & Mytilineou, C., 2019. Life-history traits of the striped red mullet *Mullus surmuletus* (Linnaeus, 1758) in the south Aegean Sea (eastern Mediterranean). *Journal of the Marine Biological Association of the United Kingdom*, 1–11.

Lauerburg, R. A. M., Keyl, F., Kotterba, P., Floeter, J., & Temming, A., 2015. Sex-specific food intake in whiting *Merlangius merlangus*. *Journal of Fish Biology*, 86 (6), 1729-1753.

Libralato, S., Caccin, A., & Pranovi, F., 2015. Modelling species invasions using thermal and trophic niche dynamics under climate change. *Frontiers in Marine Science*, 2, 29.

Lindmark, M., Ohlberger, J., & Gårdmark, A., 2022. Optimum growth temperature declines with body size within fish species. *Global Change Biology*, 28 (7), 2259-2271.

Longhurst, A., 2002. Murphy's law revisited: longevity as a factor in recruitment to fish populations. *Fisheries Research*, 56 (2), 125-131.

Lotze, H.K., Lenihan, H.S., Bourque, B.J., Bradbury, R.H., Cooke, R.G., *et al*., 2006. Depletion, degradation, and recovery potential of estuaries and coastal seas. *Science*, 312, 1806–1809.

Mehault, S., Domínguez-Petit, R., Cervino, S., & Saborido-Rey, F., 2010. Variability in total egg production and implications for management of the southern stock of European hake. *Fisheries Research*, 104 (1-3), 111-122.

Mazlum, R.E. & Bilgin, S., 2014. Age, growth, reproduction and diet of the whiting, *Merlangius merlangus euxinus* (Nordmann, 1840), in the southeastern Black Sea. *Cahiers de Biologie Marine,* 55, 463-474.

Mazzoldi, C., Sambo, A. & Riginella, E, 2014. The Clodia database: a long time series of fishery data from the Adriatic Sea. *Scientific Data*, 1, 140018. https://doi.org/10.1038/sdata.2014.18

Maximov, V., Raykov, V.S., Yankova, M., Zaharia, T., 2011. Whiting (*Merlangius merlangus euxinus*) population parameters on the Romanian and Bulgarian littoral between 2000-2008. *Journal of Environmental Protection and Ecology,* 12, 1608-1618.

Maunder, M. N., & Piner, K. R., 2014. Contemporary fisheries stock assessment: many issues still remain. *ICES Journal of Marine Science*, 72, 7–18.

Mengi, T., 1963. Uber das Wachstum des Steinbutts (*Scophthalmus maximus* L.) in der Nord see. *Berichte der Deutschen Wissenschaftlichen Kommission für Meeresforschung.* 17, 119 ± 132.

Miliić D. & Kraljević M., 2011. Biometry analysis of the whiting, *Merlangus merlangus* (Linneaus, 1758) from the northern Adriatic Sea. *Acta Adriatica*, 52: 125-136.

Murawski, S. A., Rago, P. J. & Trippel, E. A., 2001. Impacts of demographic variation in spawning characteristics on reference points for fishery management. *ICES Journal of Marine Science*, 58, 1002–1014.

Murphy, G. I., 1968. Pattern in Life History and the Environment. *The American Naturalist*, 102 (927), 391–403.

Myers, R. A., Hutchings, J. A. & Barrowman, N. J., 1997. Why do fish stocks collapse? The example of cod in Atlantic Canada. *Ecological Applications*, 7, 91–106.

O'Farrell, M. R. & Botsford, L. W., 2006a. Estimating the status of nearshore rockfish (Sebastes Spp.) populations with length frequency data. *Ecological Applicatons*, 16, 977–986.

O'Farrell, M. R. & Botsford, L. W., 2006b. The fisheries management implications of maternal-age-depedent larval survival. *Canadian Journal of Fisheries and Aquatic Sciences*, 63, 2249–2258.

Olsen, E. M., Heino, M., Lilly, G. R., Morgan, M. J., Brattey, J., Ernande, B. & Dieckmann, U., 2004. Maturation trends indicative of rapid evolution preceded the collapse of northern cod. *Nature*, 428, 932–935.

Olsen, E. M., Lilly, G. R., Heino, M., Morgan, M. J., Brattey, J. & Dieckmann, U., 2005. Assessing changes in age and size at maturation in collapsing populations of Atlantic cod (*Gadus morhua*). *Canadian Journal of Fisheries and Aquatic Sciences*, 62, 811–823.

Ottersen, G., Hjermann, D. O., Stenseth, N. C., 2006. Changes in spawning stock structure strengthen the link between climate and recruitment in a heavily fished cod (*Gadus morhua*) stock. *Fisheries Oceanography*, 15, 230–243.

Okamura, H., Punt, A. E., Semba, Y., & Ichinokawa, M., 2013. Marginal increment analysis: a new statistical approach of testing for temporal periodicity in fish age verification. *Journal of Fish Biology*, 82 (4), 1239-1249.

Panfili, J., De Pontual, H., Troadec, H. & Wright, P. J., 2002. *Manual of Fish Sclerochronology*. IRD Editore, Paris, 463 pp.

Papetti, C., Di Franco, A., Zane, L., Guidetti, P., De Simone, V., Spizzotin, M., Zorica, B., Cikeˇs Kecˇ, V., & Mazzoldi, C., 2013. Single population and common natal origin for Adriatic *Scomber scombrus* stocks: evidence from an integrated approach. *ICES Journal of Marine Science*, 70(2), 387-398.

Parker, G. A., 1992. The evolution of sexual size dimorphism in fish. *Journal of Fish Biology*, 41, 1–20.

Pauly, D., Christensen, V., Dalsgaard, J., Froese, R. & Torres, F. Jr., 1998. Fishing down marine food webs. *Science* 279, 860–863.

Pauly, D., Christensen, V., Guénette, S., Pitcher, T. J., Sumaila, R. U., Walters, C. J., Watson, R. & Zeller, D., 2002. Toward sustainability in world fisheries. *Nature*, 418, 689-695.

Penezić, A., Gašparović, B., Cuculić, V., Strmečki, S., Djakovac, T., & Mlakar, M., 2022. Dissolved trace metals and organic matter distribution in the northern Adriatic, an increasingly oligotrophic shallow sea. *Water*, 14 (3), 349.

Polat, N. & Gümüs, A., 1996. Ageing of whiting (*Merlangius merlangus euxinus*, Nord., 1840) based on broken and burnt otolith. *Fisheries Research*, 28, 231–236.

Pranovi, F., Monti, M. A., Caccin, A., Brigolin, D., & Zucchetta, M., 2015. Permanent trawl fishery closures in the Mediterranean Sea: an effective management strategy? *Marine Policy*, 60, 272-279.

Proctor, C., Robertson, S., Jatmiko, I. & Clear, N., 2021. *An introductory manual to fish ageing using otoliths,* 41 pp.

Richter, H., & McDermott, J. G., 1990. The staining of fish otoliths for age determination. *Journal of Fish Biology*, *36* (5), 773-779.

Roberts, C. M., & Hawkins, J. P., 1999. Extinction risk in the sea. *Trends in Ecology & Evolution*, 14 (6), 241-246.

Robert, F. & Vianet, R., 1988. Age and growth of *Psetta maxima* (Linné, 1758) and *Scophthalmus rhombus* (Linné, 1758) in the Gulf of Lion (Mediterranean). *Journal of Applied Ichthyology*. 4, 111 ± 120.

Roff, D. A., 1983. An allocation model of growth and reproduction in fish. *Canadian Journal of Fisheries and Aquatic Sciences*, 40 (9), 1395-1404.

Ross, S. D. & Hüssy, K., 2013. A reliable method for ageing of whiting (*Merlangius merlangus*) for use in stock assessment and management. *Journal of Applied Ichthyology*, *29* (4), 825-832.

Russo, A., & Artegiani, A., 1996. Adriatic Sea hydrography. *Scientia Marina,* 60*,* Suppl. 2, 33-43.

Şalcıoğlu, A., Gubili, C., Krey, G., Sönmez, A. Y., & Bilgin, R., 2020. Phylogeography and population dynamics of the Eastern Mediterranean whiting

(*Merlangius merlangus*) from the Black Sea, the Turkish Straits System, and the North Aegean Sea. *Fisheries Research*, 229, 105614.

Solidoro, C., Bastianini, M., Bandelj, V., Codermatz, R., Cossarini, G., Melaku Canu, D., *et al.*, 2009. Current state, scales of variability, and trends of biogeochemical properties in the northern Adriatic Sea. *Journal of Geophysical Research: Oceans*, 114 (C7).

Stagioni, M., Mazzoni, E. & Vallisneri, M., 2008. Comparazione della dieta di due Gadidi del mar Adriatico. *Biologia Marina Mediterranea*, 15(1), 358-359.

Stearns, S. C., 1976. Life-history tactics: a review of the ideas. *The Quarterly Review of Biology,* 51, 3-47.

Stearns, S., 2000. Life history evolution: successes, limitations, and prospects. *Naturwissenschaften,* 87**,** 476–486.

Szlakowski, J., 1990. Growth of *Psetta maxima* (Linnaeus, 1758) from the Gulf of Pomerania. *Acta Ichthyologica et Piscatoria,* 20, 13-28.

Tomás, J., 2006. The appearance of accessory growth centres in adult whiting *Merlangius merlangus* otoliths. *Journal of fish biology*, *69*(2), 601-607.

Vaas, K. F., Vlasblom, A. G., & De Koeijer, P., 1975. Studies on the black goby (*Gobius niger*, Gobiidae, Pisces) in the Veerse Meer, SW Netherlands. *Netherlands Journal of Sea Research*, 9 (1), 56-68.

Vallisneri, M., Vecchi, A., & Manfredi, C., 2004. The biological cycle of *Merlangius merlangus* (Linneus, 1758) (Osteichthyes, Gadidae) in the northern and middle Adriatic Sea. *Biologia Marina Mediterranea, 11(2),* 652-656.

Vallisneri, M., Scapolatempo, M., & Tommasini, S., 2006. Reproductive biology of *Merlangius merlangus* L. (Osteichthyes, Gadidae) in the northern Adriatic Sea. *Acta Adriatica*, *47*(2), 159-165.

Venturelli, P. A., Shuter, B. J., & Murphy, C. A., 2009. Evidence for harvest-induced maternal influences on the reproductive rates of fish populations. *Proceedings of the Royal Society B: Biological Sciences*, 276, 919–924.

Vitale, F., Worsøe Clausen, L., Ní Chonchúir, G. (Eds.), 2019. *Handbook of fish age estimation protocols and validation methods*. ICES Cooperative Research Report No. 346. 180 pp.

Voultsiadou, E., Koutsoubas, D., & Achparaki, M., 2010. Bivalve mollusc exploitation in Mediterranean coastal communities: an historical approach. *Journal of Biological Research*, 13, 35.

Wilhelms, I., 2013. *Atlas of length-weight relationships of 93 fish and crustacean species from the North Sea and the North-East Atlantic (No. 12)*. Johann Heinrich von Thünen Institute, Federal Research Institute for Rural Areas, Forestry and Fisheries, 552 p.

Williams, T. & Bedford, B. C., 1974. The use of otoliths for age determination. Bagenal, T. B. *ed., The ageing of fish*. Surrey, England. Unwin Brothers Ltd, The Gresham Press.

Yildiz, T., & Karakulak, F. S., 2019. Age, growth and mortality of whiting (*Merlangius merlangus*, Linnaeus, 1758) from the western Black Sea, Turkey. *Turkish Journal of Fisheries and Aquatic Sciences*, *19*(9), 793-804.

Yildiz, T., Uzer, U., Yemişken, E., Karakulak, F. S., Kahraman, A. E., & Çanak, Ö., 2021. Conserve immatures and rebound the potential: stock status and reproduction of whiting (*Merlangius merlangus* [Linnaeus, 1758]) in the Western Black Sea. *Marine Biology Research*, 17 (9-10), 815-827.

ANNEX A - Age-length Keys

1990-1991

a.

FEMALES	QUARTER												
TL 1 cm	3	6	9	12	15	18	21	24	27	30	33	36	N
12		1	1										2
13		6	2										8
14		12	6										18
15		2	4										6
16		3	4										7
17		3	4	2									9
18		3	4	2									9
19		4	4	2	1								11
20		3	4	2	2								11
21		2	4	4	2								12
22		2	3	4	2								11
23		1	3	4	2								10
24			3	3	2	1							9
25			1	2	2		1						6
26			3	7	3								13
27			1	3	5	2	1						12
28			1	2	2	1	1						7
29				1		2		1					4
30				1	1	2	1	1					6
31					1	2	1	1					5
32						2	2	3		1			8
33						1	1						2
34						1	1						2
35							1						1
37									1				1
N	-	42	52	39	25	14	10	6	1	1	-	-	190

b.

MALES	QUARTER												
TL 1 cm	3	6	9	12	15	18	21	24	27	30	33	36	N
13		5											5
14		8	7										15
15		4	4	2									10
16		2	4	2									8
17		4	4	2									10
18		4	4	3	2								13
19		4	4	4	2								14
20		2	4	6	2								14
21		2	4	5	4	1							16
22		1	4	3	3	1							12
23			4	4	4	2		1					15
24			1		3	3	1	3					11
25		1		2	1	2	2	2	1				11
26			1	1	2		2	3	1				10
27				1		2	1	2	1				7
28						2	1				1		4
29						1	1				1		3
30						1				1			2
N	-	37	45	35	23	15	8	11	3	1	2	-	180

c.

UNSEXED	QUARTER				
TL 1 cm	3	6	9	12	N
3	1				1
4	7				7
5	21				21
6	35				35
7	12				12
8	8				8
9	1	4			5
10	1	3			4
11		6			6
12		7			7
13		11	2		13
14		21	1		22
N	86	52	3	-	141

Figure 19. Age-length keys of 1990-91 females (a), males (b) and unsexed juveniles (c).

2020-2021

a.

FEMALES	QUARTER												
TL 1 cm	3	6	9	12	15	18	21	24	27	30	33	36	N
6	1												1
7	1												1
8	3	2											5
9	1	1											2
10		2											2
11		1											1
13		5											5
14		5	2	2	1								10
15		2	2	2	3								9
16		4	2	4	4								14
17		4	4	5	4	1							18
18		2	4	6	7	2							21
19		1	3	5	5	2							16
20			4	6	6	4							20
21			3	6	7	5	1						22
22			4	5	7	7							23
23			1	4	6	4	1		1				17
24				3	3	4		1	1				12
25				2	3	6	1	3	2				17
26					1	1		2	3	1			8
27						2		5	2			1	10
28						1		1				1	3
29								1				1	2
30						1		1		1			3
31								1					1
N	6	29	29	50	57	40	3	15	9	2	-	3	243

b.

MALES	QUARTER												
TL 1 cm	3	6	9	12	15	18	21	24	27	30	33	36	N
6	4												4
7	4	1											5
8	3												3
9	2												2
10	2												2
11		2											2
12		6											6
13		5			1								6
14		4		2	2								8
15		3	5	8	7	2							25
16		3	4	6	8	2							23
17		4	4	7	7	2							24
18		2	3	5	8	4							22
19			2	7	5	5							19
20			4	3	4	6	1	3	1				22
21				2	3	4	1	3	2	1			16
22						3	2	2	2	1		1	11
23					1		1	4	1				7
24						1		1	1				3
N	15	30	22	40	46	29	5	13	7	2	-	1	210

c.

UNSEXED	QUARTER				
TL 1 cm	3	6	9	12	N
4	1				1
6	8				8
7	10				10
8	5				5
9	2	1			3
N	26	1	-	-	27

Figure 20. Age-length keys of 2020-21 females (a), males (b) and unsexed juveniles (c).

ANNEX B - Von Bertalanffy curve

1990-91

a.

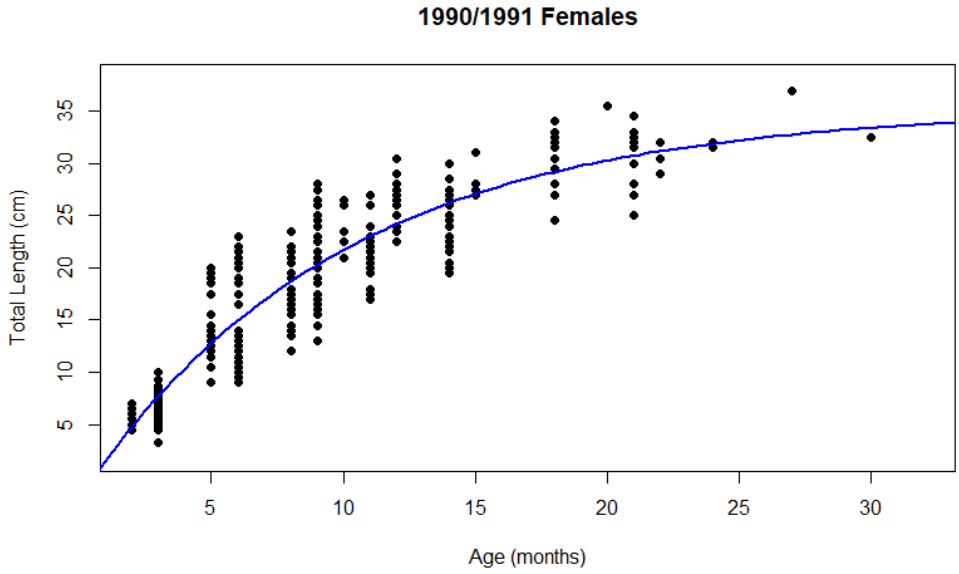

b.

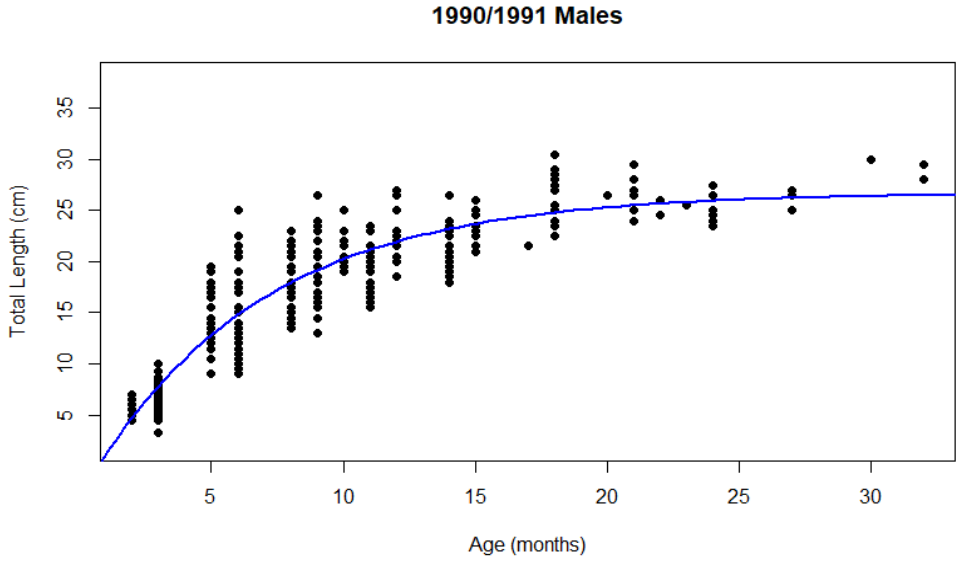

Figure 21. Von Bertalanffy curves for 1990-91 females (a) and males (b).

2020-21

a.

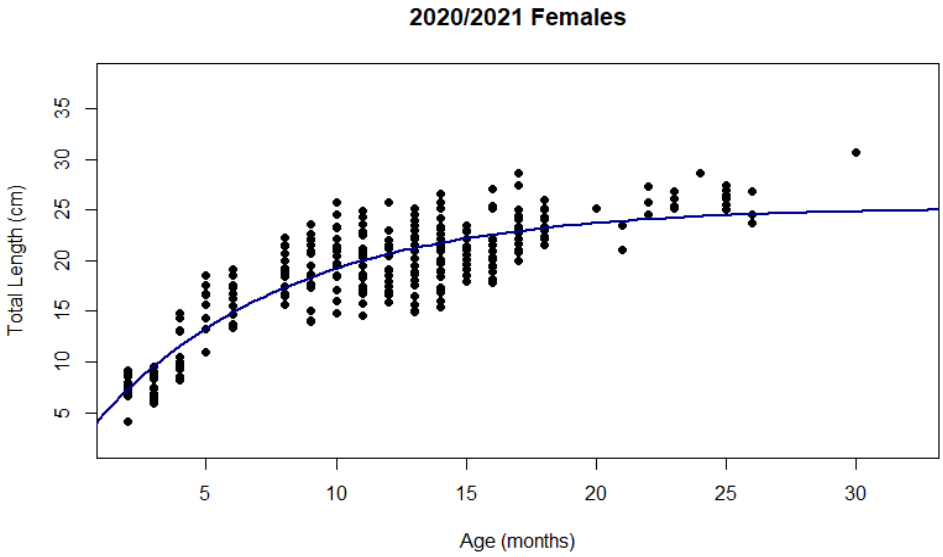

b.

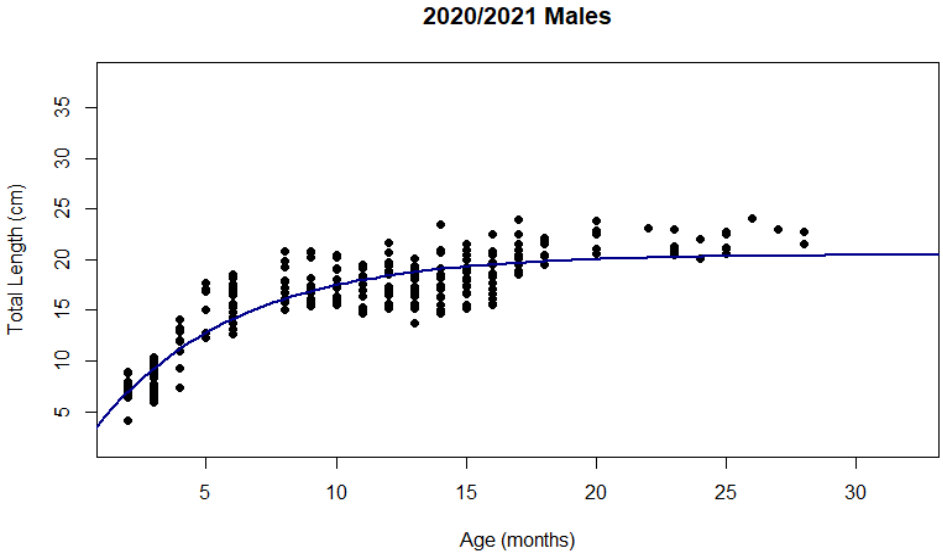

Figure 22. Von Bertalanffy curves for 2020-21 females (a) and males (b).